

SUPPORTING INFORMATION

Rupe-type Rearrangement Intercepted by Diels-Alder Cycloaddition on Osmium

Miguel A. Esteruelas, Enrique Oñate, and Sonia Paz*

Departamento de Química Inorgánica – Instituto de Síntesis Química y Catálisis Homogénea (ISQCH) – Centro de Innovación en Química Avanzada (ORFEO-CINQA), Universidad de Zaragoza – CSIC, 50009 Zaragoza, Spain

* e-mail: maester@unizar.es

Contents:

– Experimental Details	2
– Structural Analysis of Complexes 3 , 4 , 5 , 7 , and 8	3
– Computational Details.....	5
– Energies of Optimized Structures.....	6
– IR and NMR Spectra	10
– References	28

– Experimental Details

General Information.

All reactions were carried out with exclusion of air using Schlenk-tube techniques or in a glovebox. Solvents were obtained oxygen- and water-free from an MBraun solvent purification apparatus, or dried and distilled under argon prior to use. ^1H , $^{13}\text{C}\{^1\text{H}\}$, and $^{31}\text{P}\{^1\text{H}\}$ NMR spectra were recorded on Bruker 300 ARX, Bruker Avance 300 MHz, or Bruker Avance 400 MHz instruments. Chemical shifts (expressed in ppm) are referenced to residual solvent peaks (^1H , $^{13}\text{C}\{^1\text{H}\}$) and external 85% H_3PO_4 ($^{31}\text{P}\{^1\text{H}\}$) or SiMe_4 (^{29}Si). Coupling constants J and N ($N = J_{\text{P}-\text{H}} + J_{\text{P}'-\text{H}}$ for ^1H and $N = J_{\text{P}-\text{C}} + J_{\text{P}'-\text{C}}$ for $^{13}\text{C}\{^1\text{H}\}$) are given in hertz. High-resolution electrospray mass spectra were acquired using a MicroTOF-Q hybrid quadrupole time-of-flight spectrometer (Bruker Daltonics, Bremen, Germany). Attenuated total reflection infrared spectra (ATR-IR) of solid samples were run on a Perkin-Elmer Spectrum 100 FT-IR spectrometer. Elemental analyses were carried out in a Perkin-Elmer 2400-B Series II CHNS-Analyzer. $\text{Os}\{\text{C}\equiv\text{C}-\text{C}(\text{OH})\text{Ph}_2\}_2(=\text{C}=\text{C}=\text{CPh}_2)\{\kappa^3-\text{P},\text{O},\text{P}-[\text{xant}(\text{P}^i\text{Pr}_2)_2]\}(1)$ was prepared as reported previously.¹

– Structural Analysis of Complexes **3**, **4**, **5**, **7**, and **8**.

X-ray data were collected on a D8 Venture Bruker diffractometers (Mo radiation, $\lambda = 0.71073 \text{ \AA}$). The crystals were cooled with a nitrogen flow with an Oxford Cryosystems system. Data were corrected for absorption by using a multiscan method applied with the SADABS program.² The structures were solved by Patterson or direct methods and refined by full-matrix least squares on F^2 with SHELXL2019,³ including isotropic and subsequently anisotropic displacement parameters. The hydrogen atoms were observed in the last Fourier Maps or calculated, and refined freely or using a restricted riding model.

The disordered groups or solvent molecules were refined with different moieties with complementary occupancy factors and isotropic displacement parameters.

Crystal data for **3**: $C_{72}H_{71}O_2OsP_2$, BF_4 , $3(C_3H_6O)$, Mw 1481.47, violet, irregular block, $(0.122 \times 0.088 \times 0.030 \text{ mm}^3)$, monoclinic, space group $P2_1/c$, $a: 18.1573(6) \text{ \AA}$, $b: 25.7434(9) \text{ \AA}$, $c: 15.6222(4) \text{ \AA}$, $\beta: 106.4742(11)^\circ$, $V = 7002.5(4) \text{ \AA}^3$, $Z = 4$, $Z' = 1$, $D_{\text{calc}}: 1.405 \text{ g cm}^{-3}$, $F(000): 3048$, $T = 100(2) \text{ K}$, $\mu 1.930 \text{ mm}^{-1}$. 192104 measured reflections ($2\theta: 3-57^\circ$, ω and φ scans 0.5°), 17389 unique ($R_{\text{int}} = 0.0656$); min./max. transm. Factors 0.783/0.862. Final agreement factors were $R^1 = 0.0402$ (15225 observed reflections, $I > 2\sigma(I)$) and $wR^2 = 0.1034$; data/restraints/parameters 17389/27/847; GoF = 1.077. Largest peak and hole 1.247 (close to Os atoms) and -2.151 e/ \AA^3 .

Crystal data for **4**: $C_{72}H_{73}O_3OsP_2$, BF_4 , CH_2Cl_2 , Mw 1410.18, colorless, irregular block $(0.327 \times 0.129 \times 0.030 \text{ mm}^3)$, triclinic, space group $P-1$, $a: 14.9270(8) \text{ \AA}$, $b: 17.1947(10) \text{ \AA}$, $c: 25.2266(15) \text{ \AA}$, $\alpha: 83.722(3)^\circ$, $\beta: 84.203(2)^\circ$, $\gamma: 88.165(3)^\circ$, $V = 6401.6(6) \text{ \AA}^3$, $Z = 4$, $Z' = 2$, $D_{\text{calc}}: 1.463 \text{ g cm}^{-3}$, $F(000): 2872$, $T = 100(2) \text{ K}$, $\mu 2.185 \text{ mm}^{-1}$. 367266 measured reflections ($2\theta: 3-57^\circ$, ω and φ scans 0.5°), 23775 unique ($R_{\text{int}} = 0.0612$); min./max. transm. Factors 0.746/0.995. Final agreement factors were $R^1 = 0.0807$ (21802 observed

reflections, $I > 2\sigma(I)$) and $wR^2 = 0.1869$; data/restraints/parameters 23775/37/1526; GoF = 1.186. Largest peak and hole 4.683 (close to Os atoms) and -3.476 e/ Å³.

Crystal data for **5**: C₇₂H₇₂FO₂OsP₂, BF₄, 0.5(CH₂Cl₂), Mw 1369.70, red, needle, (0.500 x 0.026 x 0.020 mm³), monoclinic, space group P2₁/c, *a*: 23.994(2) Å, *b*: 16.2114(13) Å, *c*: 16.3311(13) Å, β : 101.817(3)°, *V* = 6217.8(9) Å³, *Z* = 4, *Z'* = 1, D_{calc}: 1.463 g cm⁻³, F(000): 2788, T = 100(2) K, μ 2.207 mm⁻¹. 247666 measured reflections (2θ: 3-51°, ω and φ scans 0.5°), 15478 unique (R_{int} = 0.0761); min./max. transm. Factors 0.744/0.862. Final agreement factors were R¹ = 0.0589 (12638 observed reflections, $I > 2\sigma(I)$) and wR^2 = 0.1342; data/restraints/parameters 15478/18/779; GoF = 1.123. Largest peak and hole 2.407 (close to Os atoms) and -3.303 e/ Å³.

Crystal data for **7**: C₇₂H₇₀FOOsP₂, BF₄, 2(CH₂Cl₂), Mw 1479.08, red, irregular block, (0.136 x 0.110 x 0.053 mm³), triclinic, P-1, *a*: 11.9505(7) Å, *b*: 15.6156(9) Å, *c*: 18.3174(11) Å, α : 81.225(2)°, β : 78.772(2)°, γ : 86.447(2)°, *V* = 3311.8(3) Å³, *Z* = 2, *Z'* = 1, D_{calc}: 1.483 g cm⁻³, F(000): 1500, T = 100(2) K, μ 2.194 mm⁻¹. 182259 measured reflections (2θ: 3-57°, ω and φ scans 0.5°), 16494 unique (R_{int} = 0.0335); min./max. transm. Factors 0.672/0.746. Final agreement factors were R¹ = 0.0606 (16174 observed reflections, $I > 2\sigma(I)$) and wR^2 = 0.1461; data/restraints/parameters 16494/12/ 788; GoF = 1.287. Largest peak and hole 3.924 (close to Os atoms) and -3.925 e/ Å³.

Crystal data for **8**: C₇₂H₇₁F₂OOsP₂, BF₄, 1.875(CH₂Cl₂), Mw 1488.47, yellow, needle (0.400 x 0.040 x 0.020 mm³), monoclinic, space group P2₁/n, *a*: 16.2747(7) Å, *b*: 36.7648(15) Å, *c*: 22.7232(8) Å, β : 99.0568(16)°, *V* = 13426.6(9) Å³, *Z* = 8, *Z'* = 2, D_{calc}: 1.473 g cm⁻³, F(000): 6038, T = 100(2) K, μ 2.157 mm⁻¹. 455810 measured reflections (2θ: 3-57°, ω and φ scans 0.5°), 33370 unique (R_{int} = 0.0777); min./max. transm. Factors 0.729/0.862. Final agreement factors were R¹ = 0.0669 (27323 observed reflections, $I >$

$2\sigma(I)$) and $wR^2 = 0.1899$; data/restraints/parameters 33370/81/1450; GoF = 1.075.

Largest peak and hole 4.921 (close to Os atoms) and -3.019 e/ Å³.

– Computational Details.

All calculations were performed at the DFT level using the B3LYP functional⁴ supplemented with the Grimme's dispersion correction D3⁵ as implemented in Gaussian09.⁶ Os atoms were described by means of an effective core potential SDD for the inner electron⁷ and its associated double- ζ basis set for the outer ones, complemented with a set of f-polarization functions for osmium.⁸ The 6-31G** basis set was used for all the other atoms.⁹ Reactants, intermediates, and products were also characterized by frequency calculations and has positive definite Hessian matrices thus confirming that the computed structure is a minimum on the potential energy surface. Transition states were identified by having one imaginary frequency in the Hessian matrix. It was confirmed that transition states connect with the corresponding intermediates by means of application of an eigenvector corresponding to the imaginary frequency and subsequent optimization of the resulting structures. Gibbs energies were computed at 298.15 K and 1 atmosphere. All values collected in schemes and figures correspond to Gibbs energies in dichloromethane in kcal mol⁻¹.

– Energies of Optimized Structures

Complex 5:

Zero-point correction=	1.244219 (Hartree/Particle)
Thermal correction to Energy=	1.319366
Thermal correction to Enthalpy=	1.320311
Thermal correction to Gibbs Free Energy=	1.131983
Sum of electronic and zero-point Energies=	-3809.793349
Sum of electronic and thermal Energies=	-3809.718202
Sum of electronic and thermal Enthalpies=	-3809.717258
Sum of electronic and thermal Free Energies=	-3809.905586

Complex TS(5-9t):

Zero-point correction=	1.256318 (Hartree/Particle)
Thermal correction to Energy=	1.331058
Thermal correction to Enthalpy=	1.332002
Thermal correction to Gibbs Free Energy=	1.145069
Sum of electronic and zero-point Energies=	-3810.206338
Sum of electronic and thermal Energies=	-3810.131597
Sum of electronic and thermal Enthalpies=	-3810.130653
Sum of electronic and thermal Free Energies=	-3810.317586

Complex 9t:

Zero-point correction=	1.230114 (Hartree/Particle)
Thermal correction to Energy=	1.304115
Thermal correction to Enthalpy=	1.305060
Thermal correction to Gibbs Free Energy=	1.118153
Sum of electronic and zero-point Energies=	-3733.798444
Sum of electronic and thermal Energies=	-3733.724443
Sum of electronic and thermal Enthalpies=	-3733.723499
Sum of electronic and thermal Free Energies=	-3733.910405

Complex TS(9t-10t):

Zero-point correction=	1.230567 (Hartree/Particle)
Thermal correction to Energy=	1.303129
Thermal correction to Enthalpy=	1.304073
Thermal correction to Gibbs Free Energy=	1.123847
Sum of electronic and zero-point Energies=	-3733.776305
Sum of electronic and thermal Energies=	-3733.703743
Sum of electronic and thermal Enthalpies=	-3733.702799
Sum of electronic and thermal Free Energies=	-3733.883025

Complex 10t:

Zero-point correction=	1.231046 (Hartree/Particle)
Thermal correction to Energy=	1.303816

Thermal correction to Enthalpy=	1.304760
Thermal correction to Gibbs Free Energy=	1.124136
Sum of electronic and zero-point Energies=	-3733.782223
Sum of electronic and thermal Energies=	-3733.709453
Sum of electronic and thermal Enthalpies=	-3733.708509
Sum of electronic and thermal Free Energies=	-3733.889133

Complex 11t:

Zero-point correction=	1.220576 (Hartree/Particle)
Thermal correction to Energy=	1.292705
Thermal correction to Enthalpy=	1.293650
Thermal correction to Gibbs Free Energy=	1.113900
Sum of electronic and zero-point Energies=	-3733.412429
Sum of electronic and thermal Energies=	-3733.340300
Sum of electronic and thermal Enthalpies=	-3733.339356
Sum of electronic and thermal Free Energies=	-3733.519105

Complex TS(11t-7):

Zero-point correction=	1.219309 (Hartree/Particle)
Thermal correction to Energy=	1.291029
Thermal correction to Enthalpy=	1.291973
Thermal correction to Gibbs Free Energy=	1.112484
Sum of electronic and zero-point Energies=	-3733.407700
Sum of electronic and thermal Energies=	-3733.335979
Sum of electronic and thermal Enthalpies=	-3733.335035
Sum of electronic and thermal Free Energies=	-3733.514524

Complex 7:

Zero-point correction=	1.221604 (Hartree/Particle)
Thermal correction to Energy=	1.293115
Thermal correction to Enthalpy=	1.294060
Thermal correction to Gibbs Free Energy=	1.116723
Sum of electronic and zero-point Energies=	-3733.430573
Sum of electronic and thermal Energies=	-3733.359061
Sum of electronic and thermal Enthalpies=	-3733.358117
Sum of electronic and thermal Free Energies=	-3733.535454

Complex TS(11t-12t):

Zero-point correction=	1.245331 (Hartree/Particle)
Thermal correction to Energy=	1.318761
Thermal correction to Enthalpy=	1.319705
Thermal correction to Gibbs Free Energy=	1.137879
Sum of electronic and zero-point Energies=	-3809.832469
Sum of electronic and thermal Energies=	-3809.759040
Sum of electronic and thermal Enthalpies=	-3809.758095
Sum of electronic and thermal Free Energies=	-3809.939921

Complex 12t:

Zero-point correction=	1.246651 (Hartree/Particle)
Thermal correction to Energy=	1.319944
Thermal correction to Enthalpy=	1.320888
Thermal correction to Gibbs Free Energy=	1.139656
Sum of electronic and zero-point Energies=	-3809.854341
Sum of electronic and thermal Energies=	-3809.781049
Sum of electronic and thermal Enthalpies=	-3809.780104
Sum of electronic and thermal Free Energies=	-3809.961336

Complex 13t:

Zero-point correction=	1.247080 (Hartree/Particle)
Thermal correction to Energy=	1.320892
Thermal correction to Enthalpy=	1.321837
Thermal correction to Gibbs Free Energy=	1.139486
Sum of electronic and zero-point Energies=	-3809.869944
Sum of electronic and thermal Energies=	-3809.796131
Sum of electronic and thermal Enthalpies=	-3809.795187
Sum of electronic and thermal Free Energies=	-3809.977538

Complex TS(13t-3):

Zero-point correction=	1.243987 (Hartree/Particle)
Thermal correction to Energy=	1.316535
Thermal correction to Enthalpy=	1.317479
Thermal correction to Gibbs Free Energy=	1.137914
Sum of electronic and zero-point Energies=	-3809.848257
Sum of electronic and thermal Energies=	-3809.775709
Sum of electronic and thermal Enthalpies=	-3809.774765
Sum of electronic and thermal Free Energies=	-3809.954330

Complex 3:

Zero-point correction=	1.235667 (Hartree/Particle)
Thermal correction to Energy=	1.307093
Thermal correction to Enthalpy=	1.308037
Thermal correction to Gibbs Free Energy=	1.129569
Sum of electronic and zero-point Energies=	-3709.455236
Sum of electronic and thermal Energies=	-3709.383810
Sum of electronic and thermal Enthalpies=	-3709.382866
Sum of electronic and thermal Free Energies=	-3709.561334

HF:

Zero-point correction=	0.009154 (Hartree/Particle)
Thermal correction to Energy=	0.011515
Thermal correction to Enthalpy=	0.012459

Thermal correction to Gibbs Free Energy=	-0.007269
Sum of electronic and zero-point Energies=	-100.425448
Sum of electronic and thermal Energies=	-100.423088
Sum of electronic and thermal Enthalpies=	-100.422144
Sum of electronic and thermal Free Energies=	-100.441871

BF₄⁻:

Zero-point correction=	0.014210 (Hartree/Particle)
Thermal correction to Energy=	0.018633
Thermal correction to Enthalpy=	0.019577
Thermal correction to Gibbs Free Energy=	-0.011099
Sum of electronic and zero-point Energies=	-424.574122
Sum of electronic and thermal Energies=	-424.569699
Sum of electronic and thermal Enthalpies=	-424.568755
Sum of electronic and thermal Free Energies=	-424.599431

HBF₄:

Zero-point correction=	0.023363 (Hartree/Particle)
Thermal correction to Energy=	0.029720
Thermal correction to Enthalpy=	0.030664
Thermal correction to Gibbs Free Energy=	-0.006763
Sum of electronic and zero-point Energies=	-424.981710
Sum of electronic and thermal Energies=	-424.975353
Sum of electronic and thermal Enthalpies=	-424.974409
Sum of electronic and thermal Free Energies=	-425.011837

H₂O:

Zero-point correction=	0.021133 (Hartree/Particle)
Thermal correction to Energy=	0.023968
Thermal correction to Enthalpy=	0.024912
Thermal correction to Gibbs Free Energy=	0.003467
Sum of electronic and zero-point Energies=	-76.405573
Sum of electronic and thermal Energies=	-76.402738
Sum of electronic and thermal Enthalpies=	-76.401794
Sum of electronic and thermal Free Energies=	-76.423239

- IR and NMR Spectra

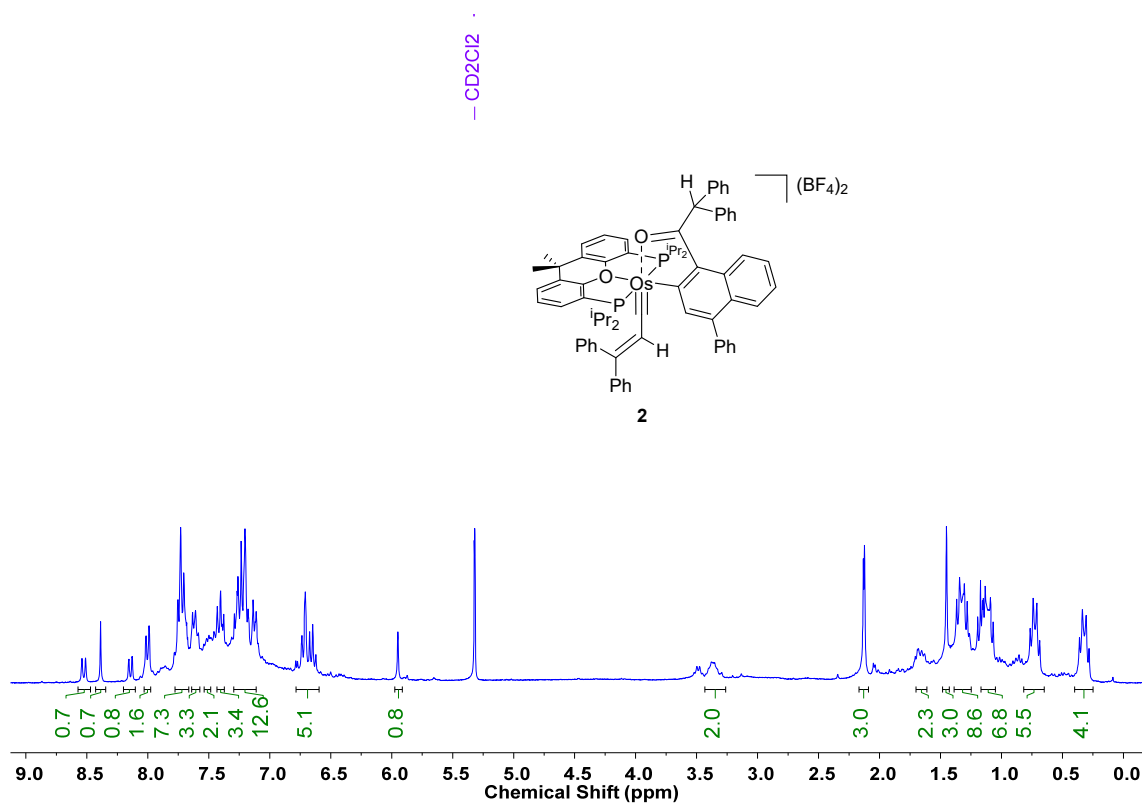


Figure S1. ^1H NMR spectrum (300.13 MHz, CD_2Cl_2 , 298 K) of **2**.

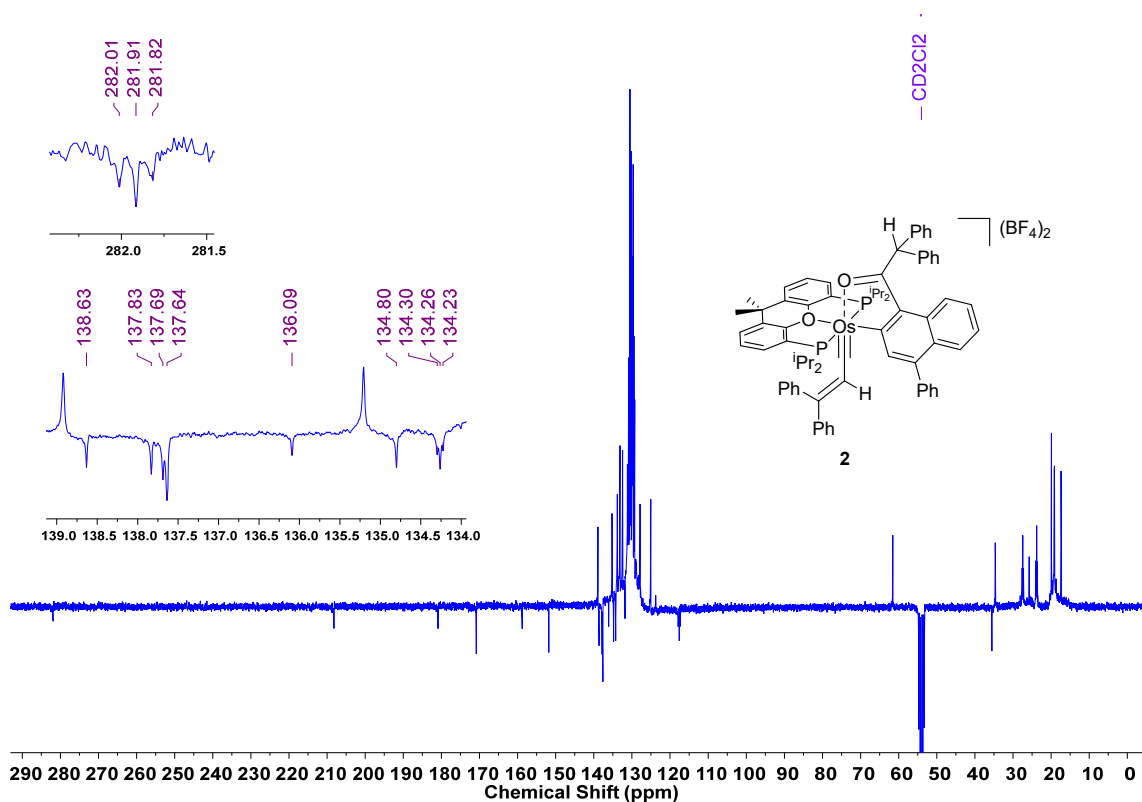


Figure S2. $^{13}\text{C}\{^1\text{H}\}$ -APT NMR spectrum (75.48 MHz, CD_2Cl_2 , 298 K) of 2.

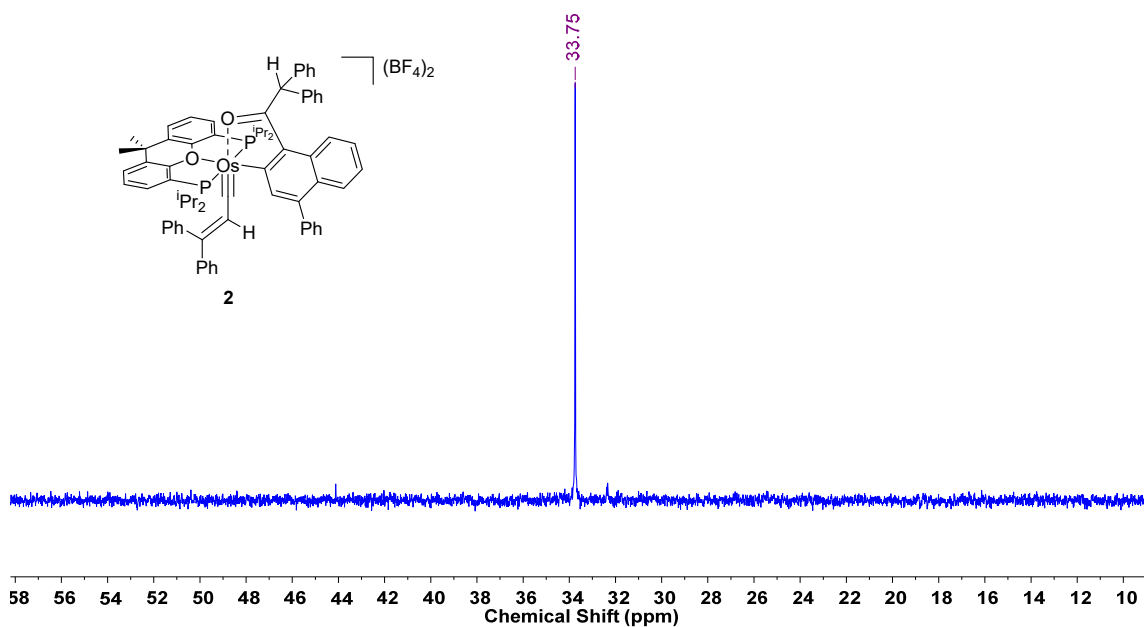


Figure S3. $^{31}\text{P}\{\text{H}\}$ NMR spectrum (121.49 MHz, CD₂Cl₂, 298 K) of **2**.

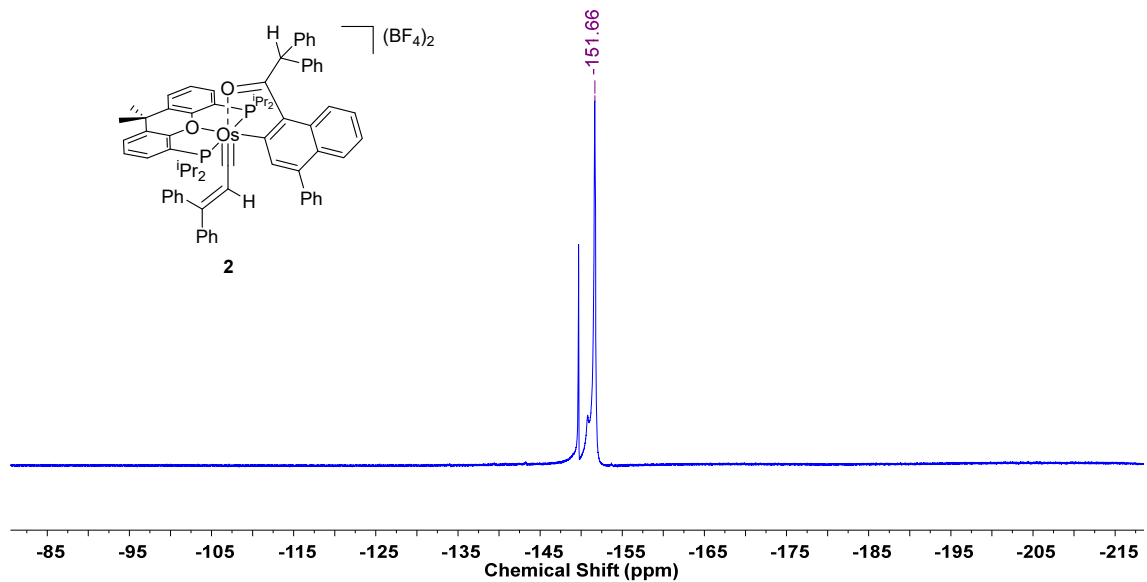


Figure S4. $^{19}\text{F}\{\text{H}\}$ NMR spectrum (282.38 MHz, CD₂Cl₂, 298 K) of **2**.

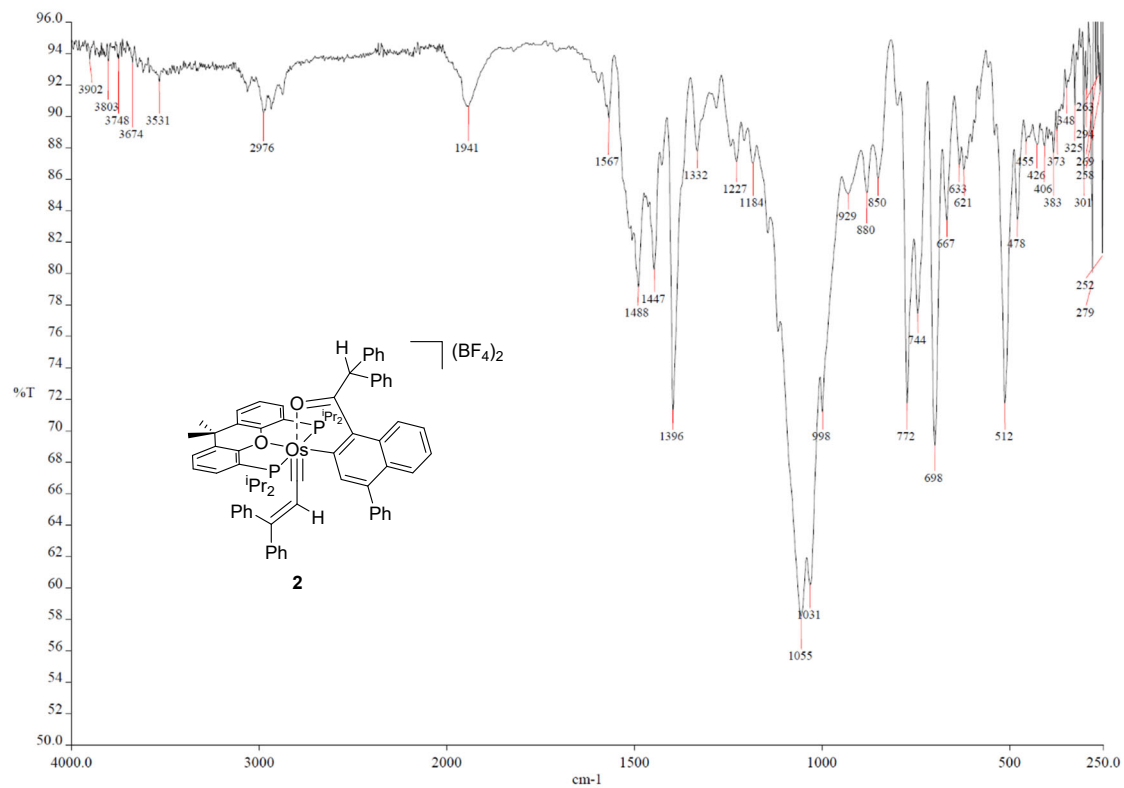


Figure S5. ATR-IR spectrum of **2**.

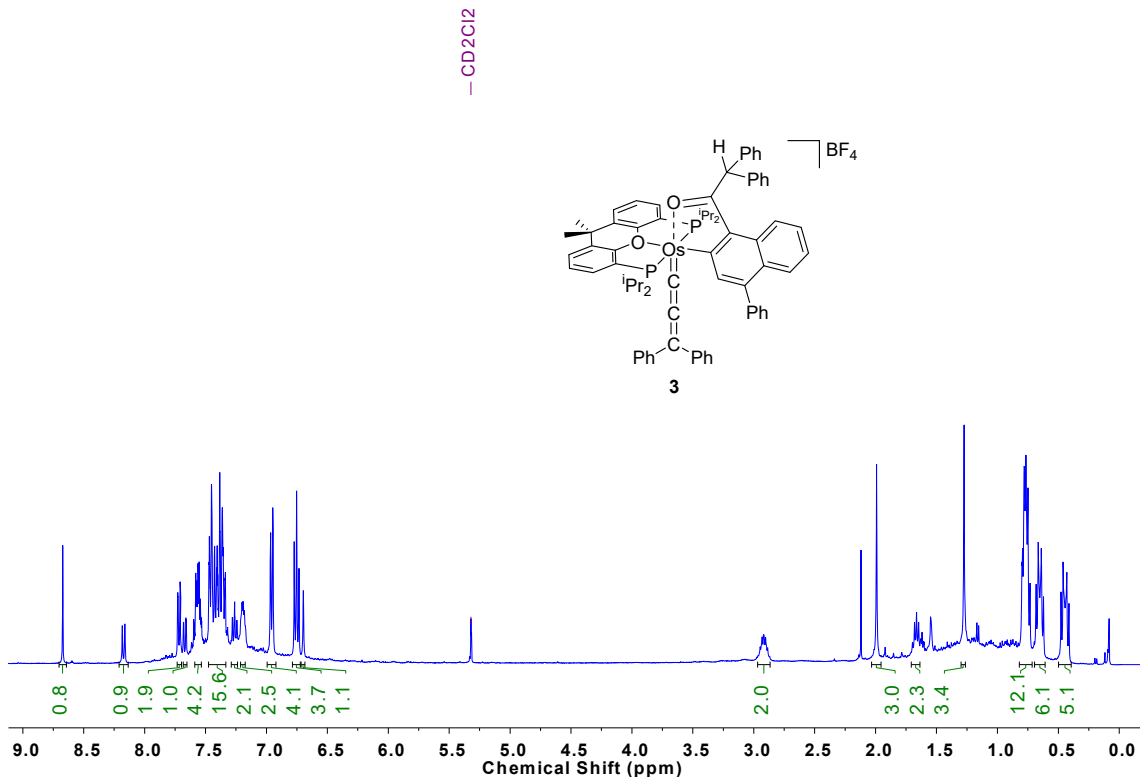


Figure S6. ^1H NMR spectrum (400.13 MHz, CD_2Cl_2 , 298 K) of **3**.

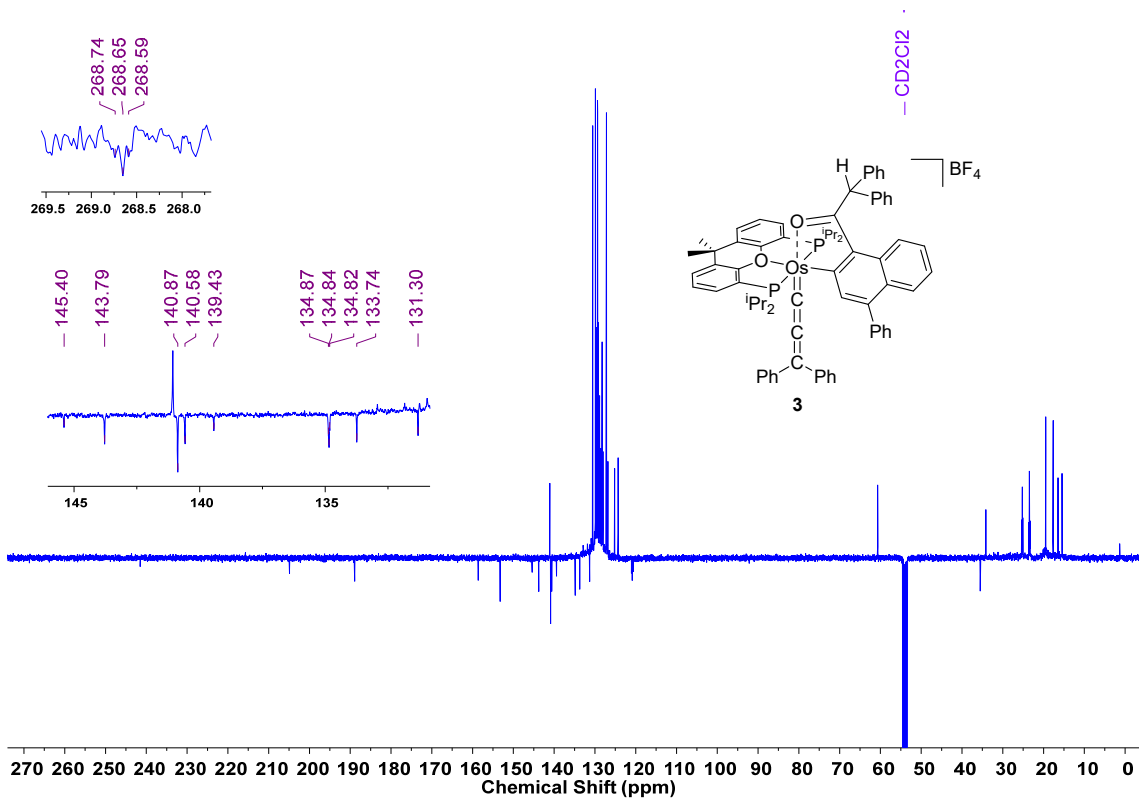


Figure S7. $^{13}\text{C}\{^1\text{H}\}$ -APT NMR spectrum (100.62 MHz, CD_2Cl_2 , 298 K) of **3**.

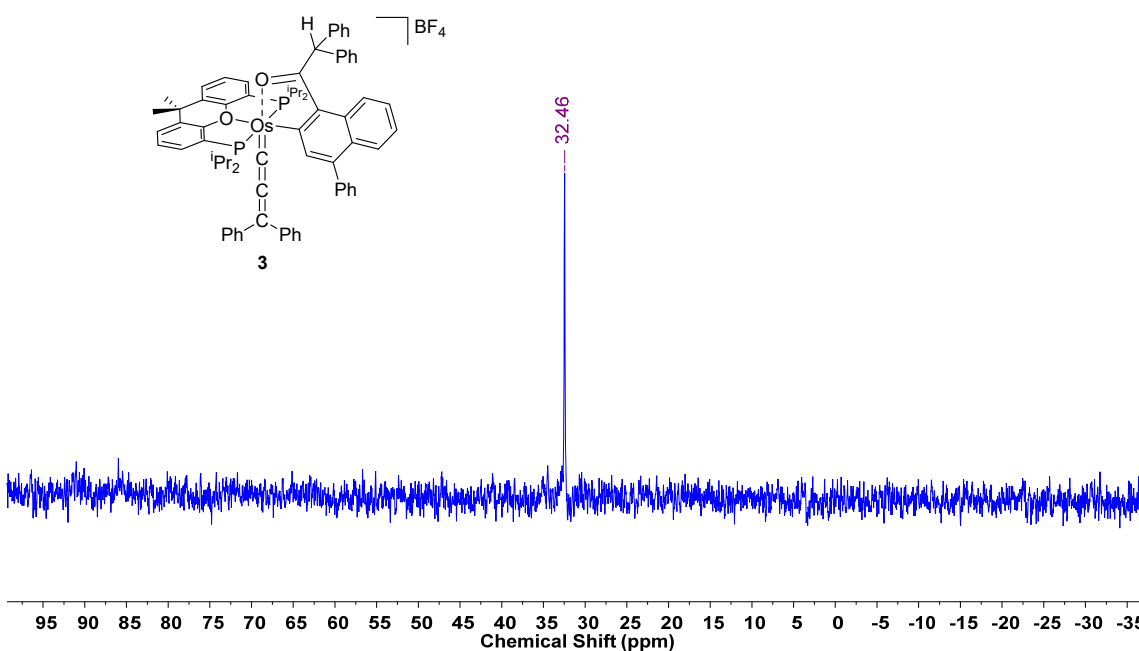


Figure S8. $^{31}\text{P}\{^1\text{H}\}$ NMR spectrum (121.49 MHz, CD_2Cl_2 , 298 K) of **3**.

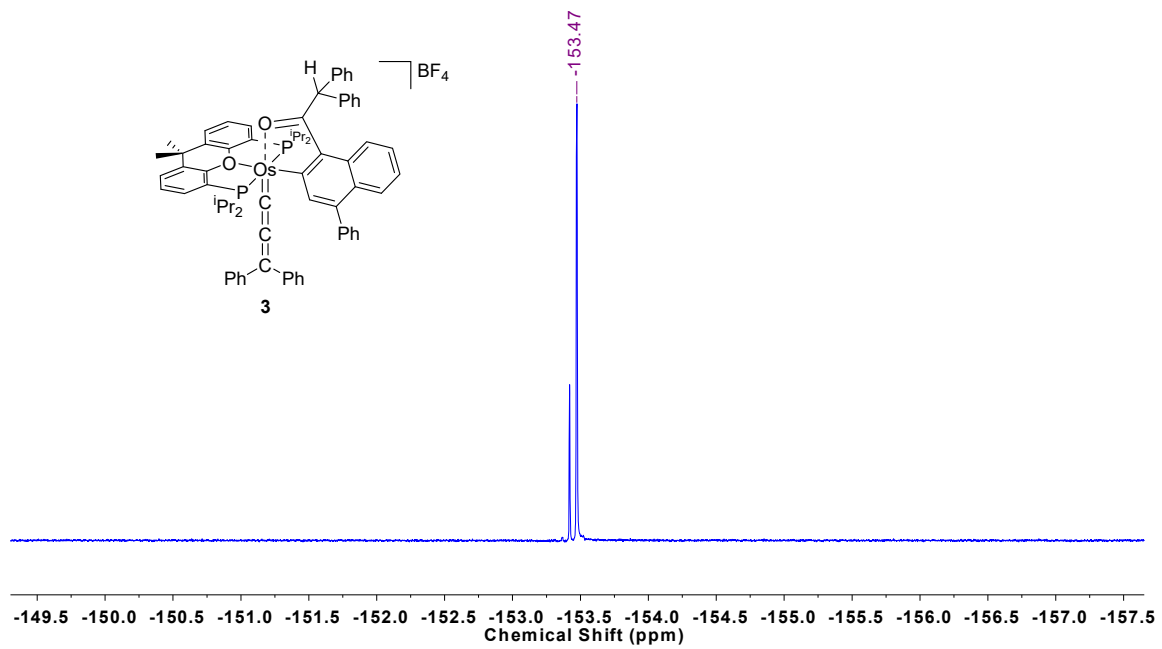


Figure S9. ¹⁹F{¹H} NMR spectrum (376.44 MHz, CD₂Cl₂, 298 K) of **3**.

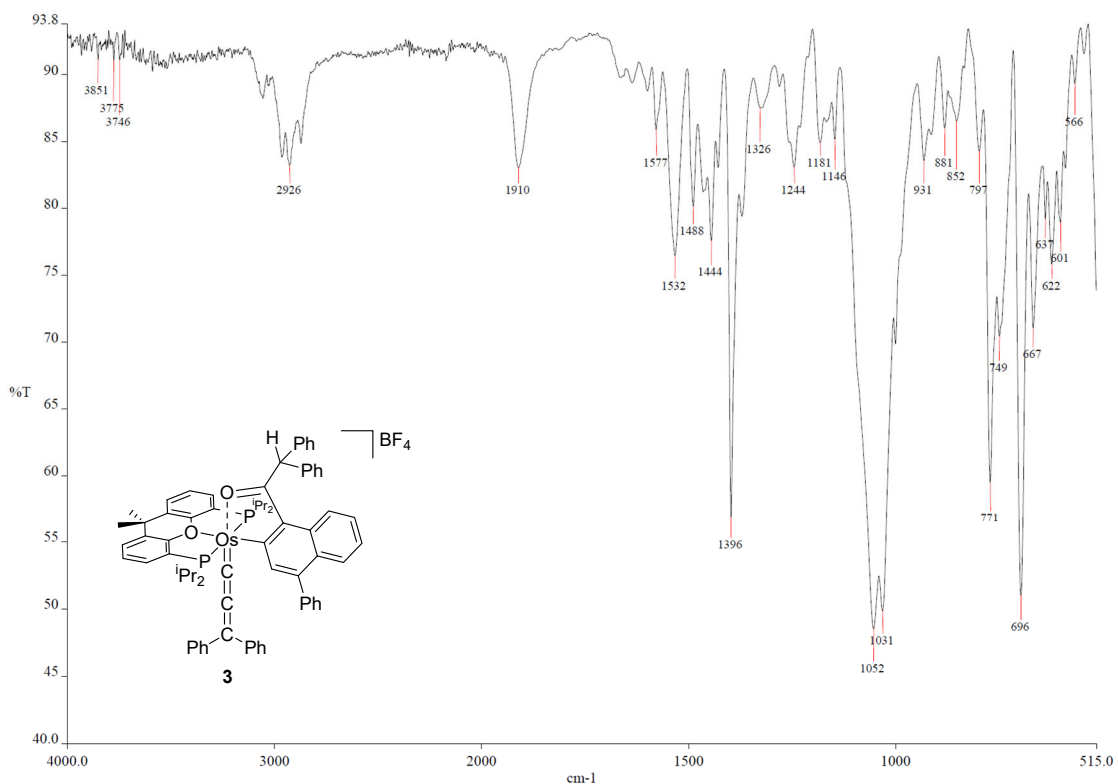


Figure S10. ATR-IR spectrum of **3**.

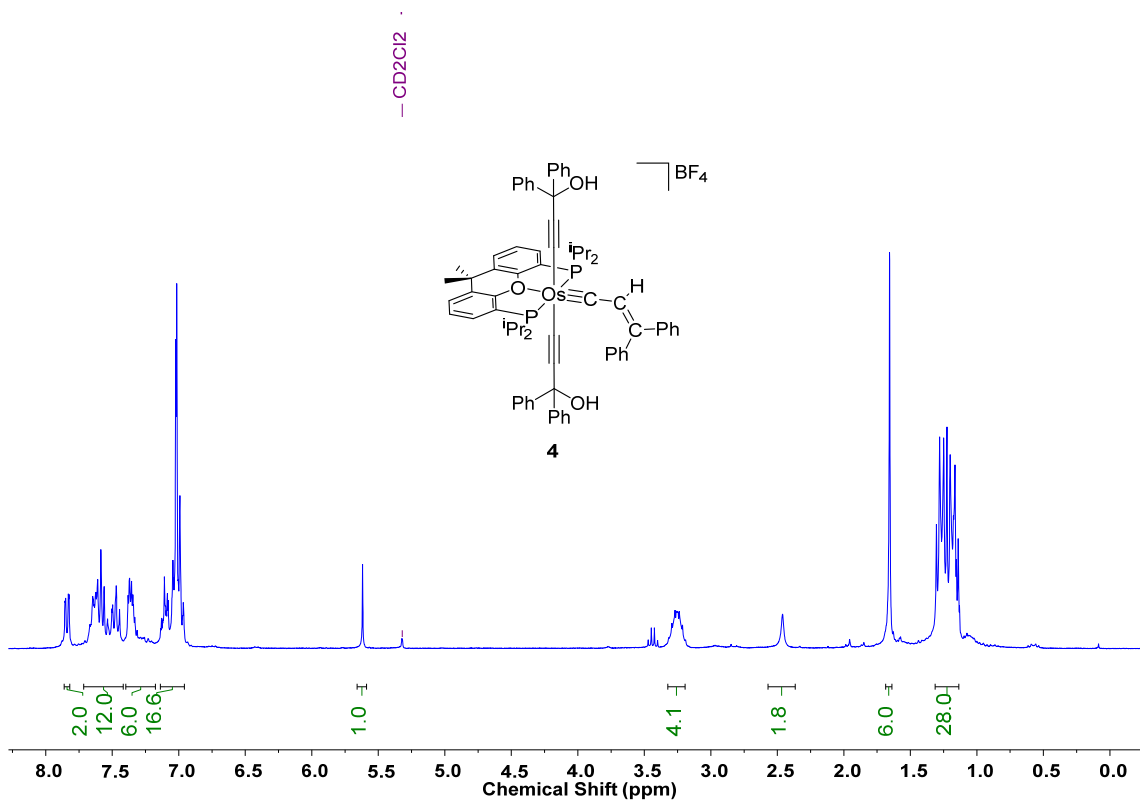


Figure S11. ^1H NMR spectrum (300.13 MHz, CD_2Cl_2 , 298 K) of **4**.

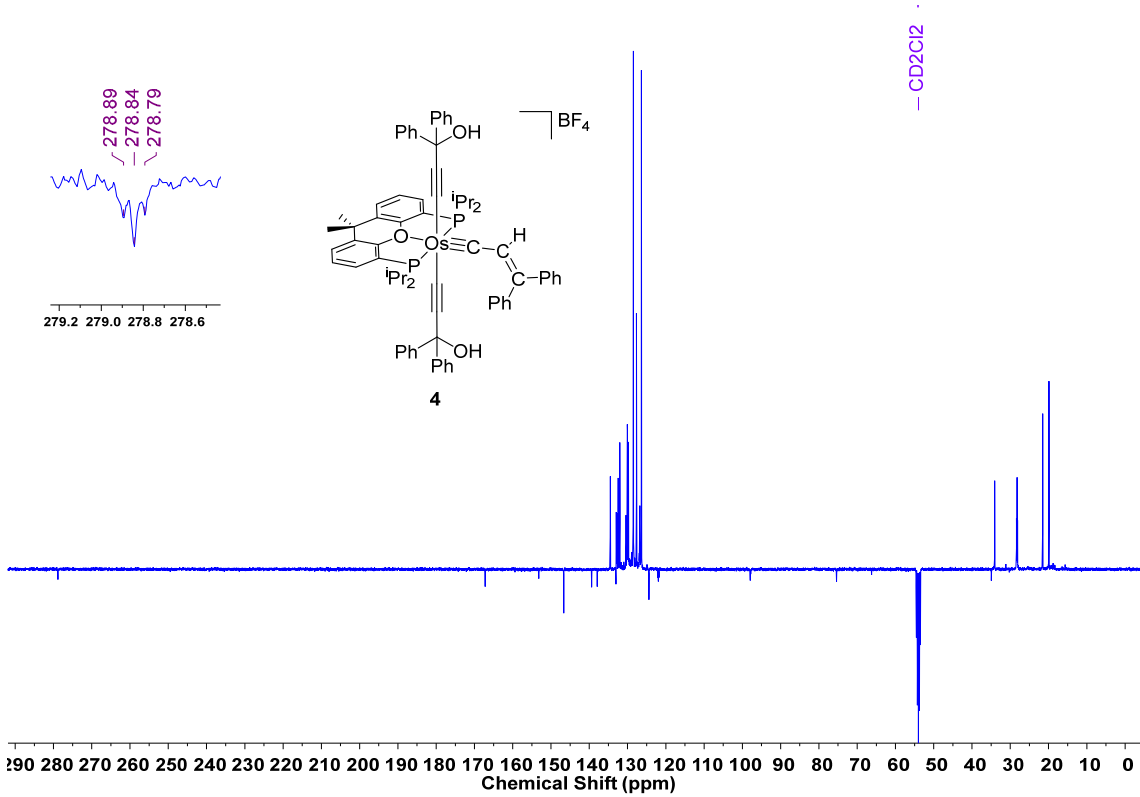


Figure S12. $^{13}\text{C}\{^1\text{H}\}$ -APT NMR spectrum (100.62 MHz, CD_2Cl_2 , 298 K) of **4**.

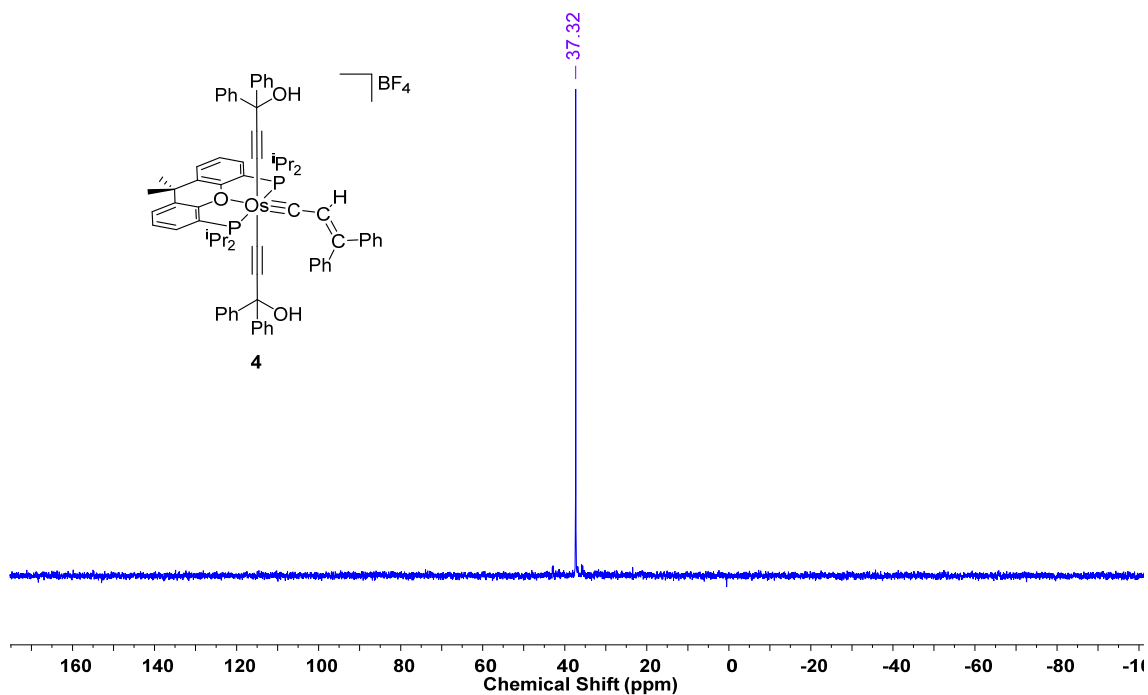


Figure S13. ³¹P{¹H} NMR spectrum (121.49 MHz, CD₂Cl₂, 298 K) of **4**.

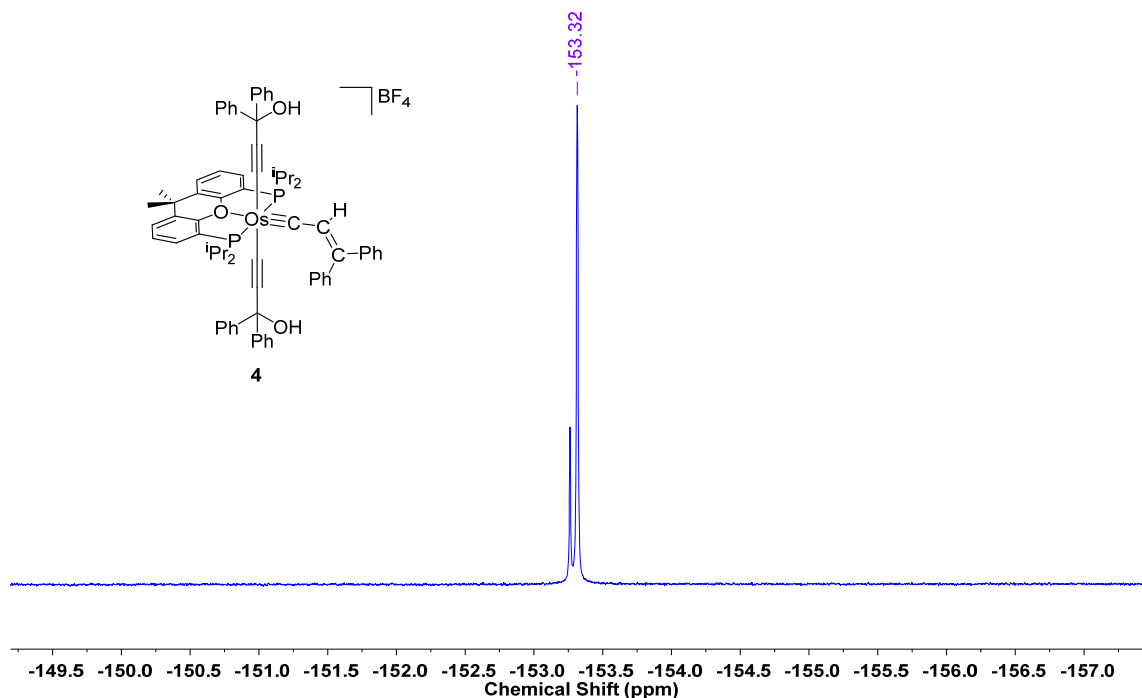


Figure S14. ¹⁹F{¹H} NMR spectrum (376.44 MHz, CD₂Cl₂, 298 K) of **4**.

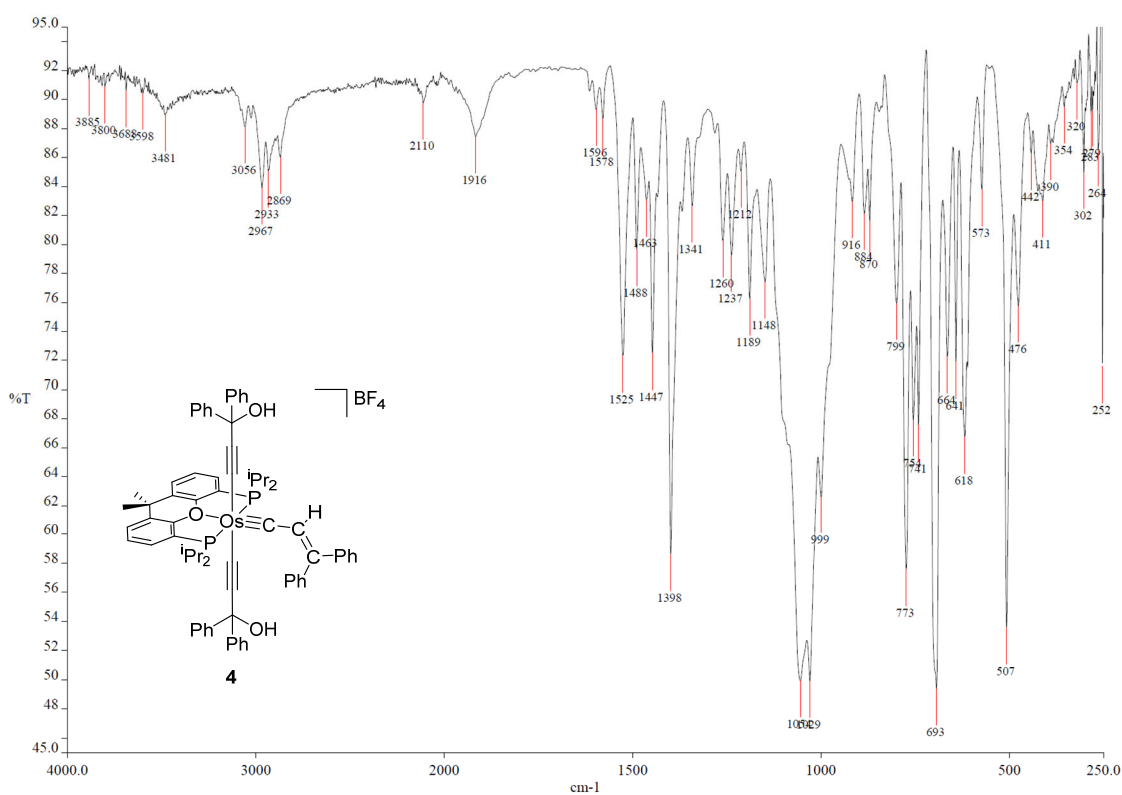


Figure S15. ATR-IR spectrum of **4**.

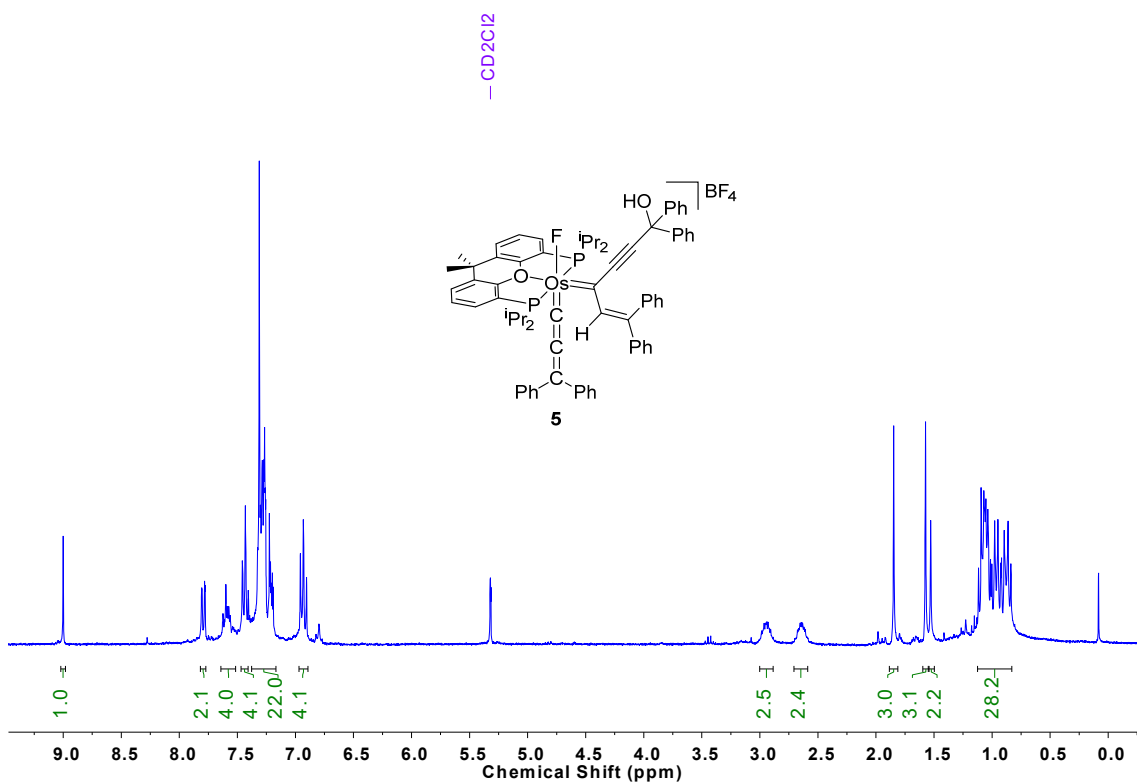


Figure S16. ^1H NMR spectrum (300.13 MHz, CD_2Cl_2 , 298 K) of **5**.

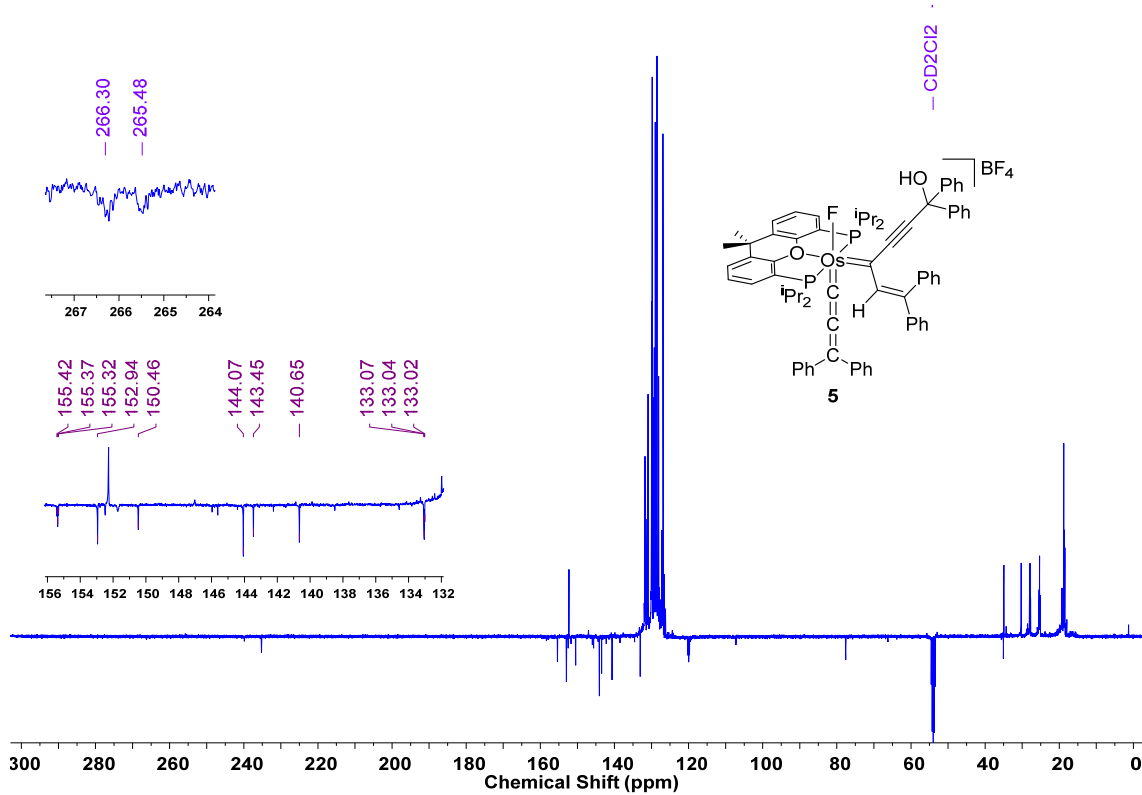


Figure S17. $^{13}\text{C}\{^1\text{H}\}$ -APT NMR spectrum (100.62 MHz, CD_2Cl_2 , 298 K) of **5**.

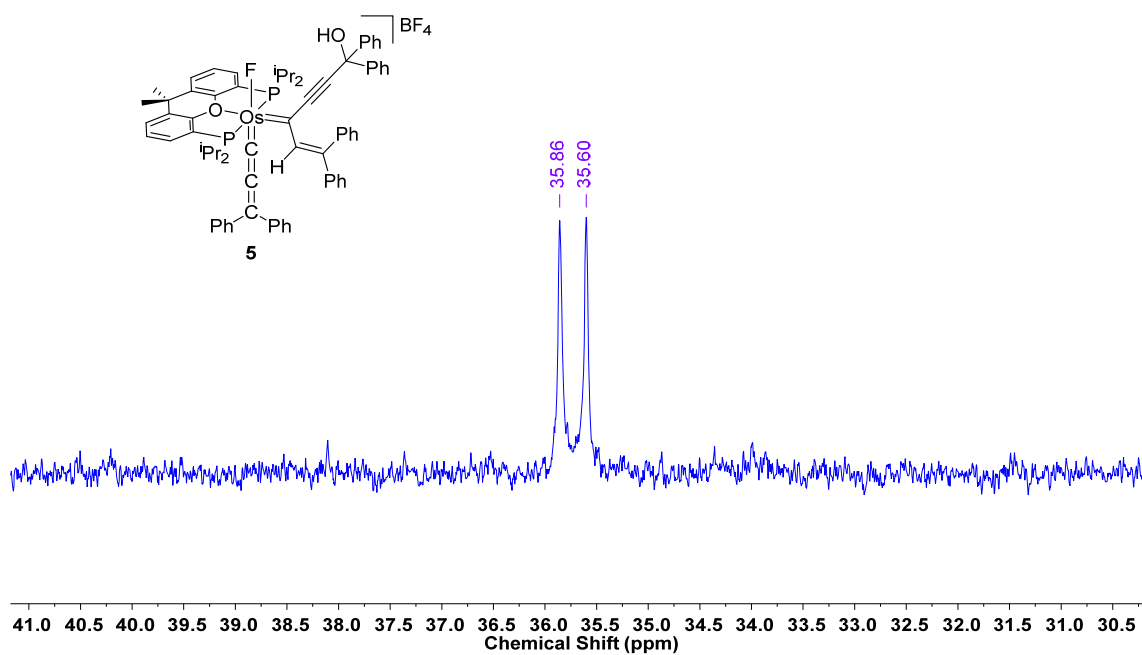


Figure S18. $^{31}\text{P}\{^1\text{H}\}$ NMR spectrum (121.49 MHz, CD_2Cl_2 , 298 K) of **5**.

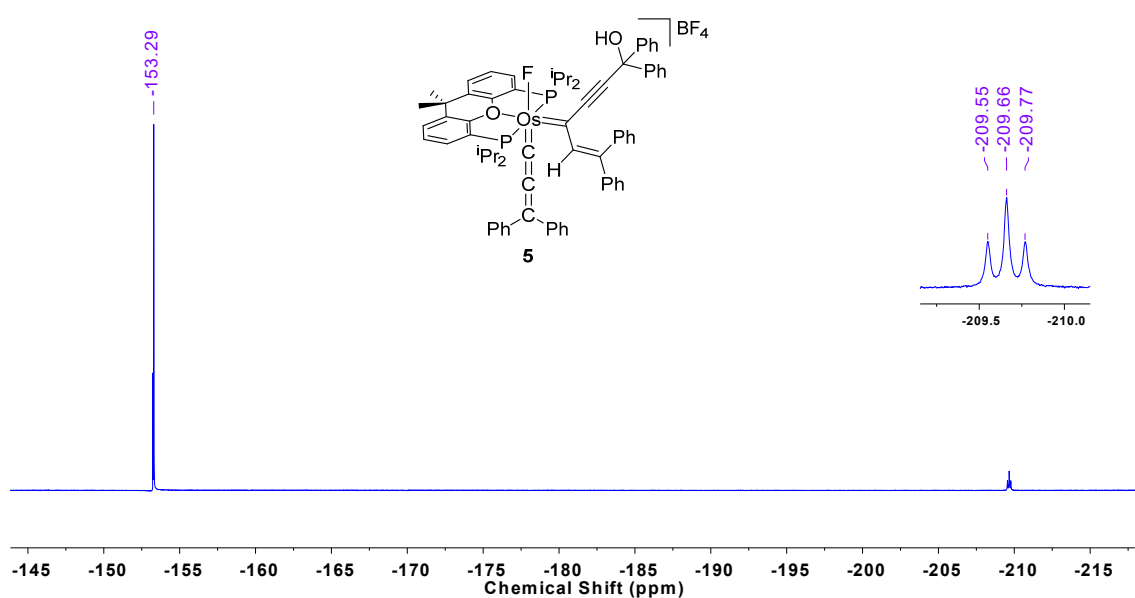


Figure S19. $^{19}\text{F}\{^1\text{H}\}$ NMR spectrum (282.38 MHz, CD_2Cl_2 , 298 K) of **5**.

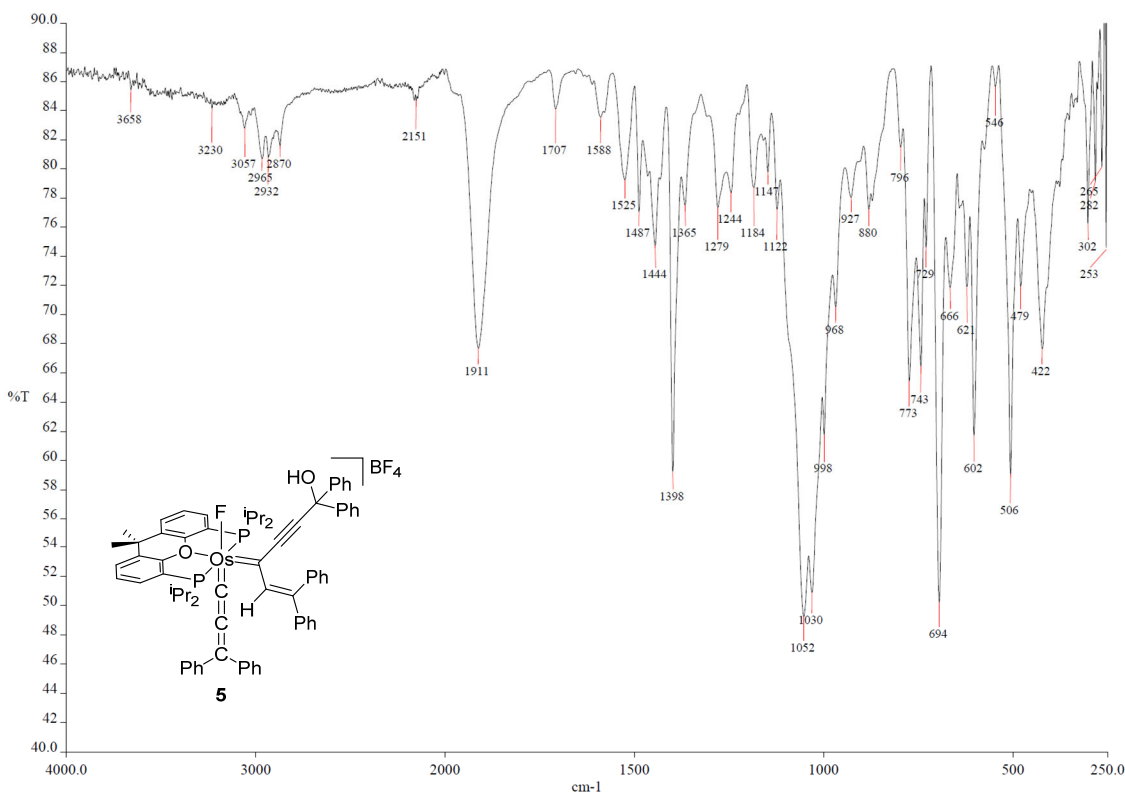


Figure S20. ATR-IR spectrum of **5**.

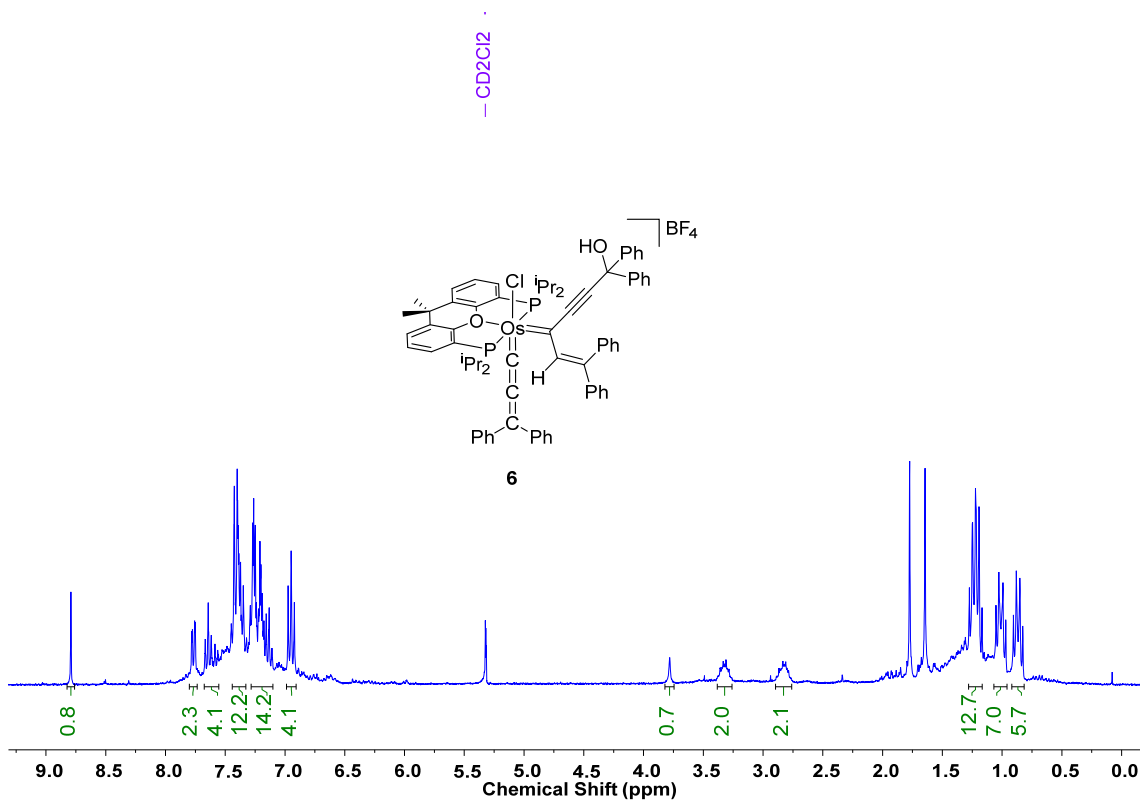


Figure S21. ^1H NMR spectrum (300.13 MHz, CD₂Cl₂, 298 K) of **6**.

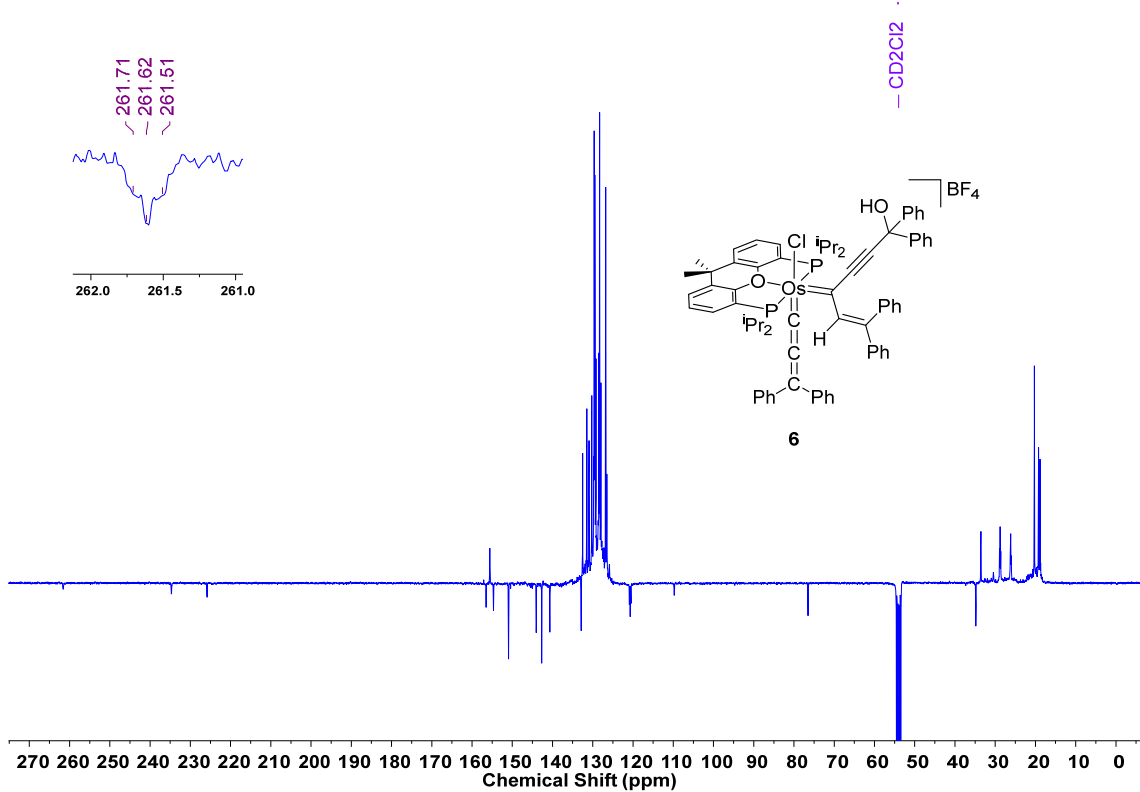


Figure S22. $^{13}\text{C}\{^1\text{H}\}$ -APT NMR spectrum (100.62 MHz, CD₂Cl₂, 253 K) of **6**.

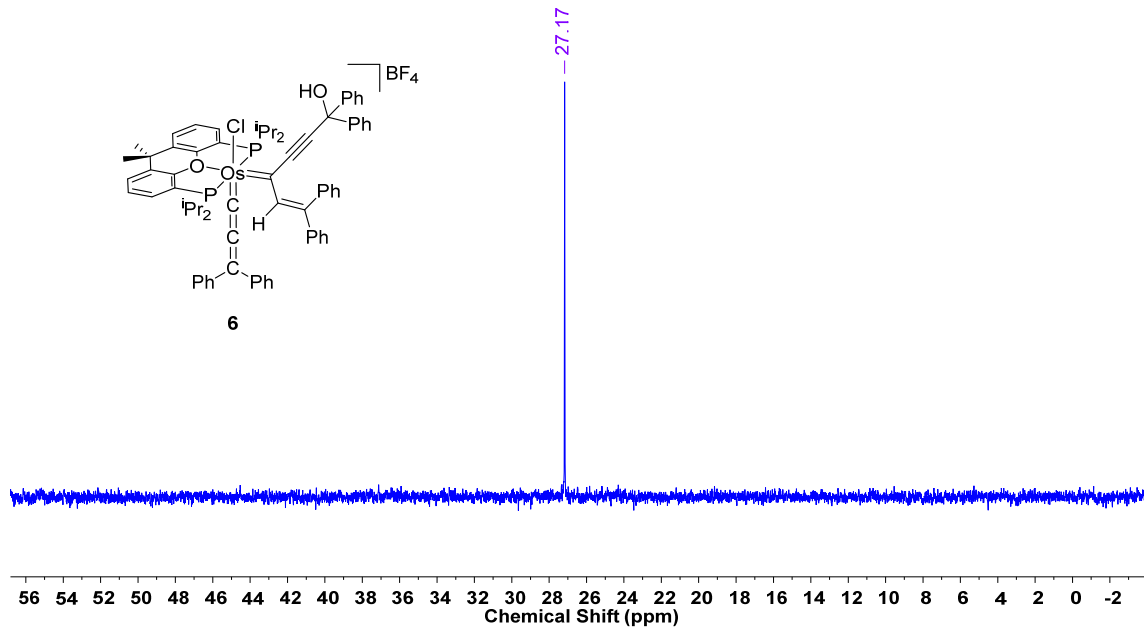


Figure S23. $^{31}\text{P}\{\text{H}\}$ NMR spectrum (121.49 MHz, CD_2Cl_2 , 298 K) of **6**.

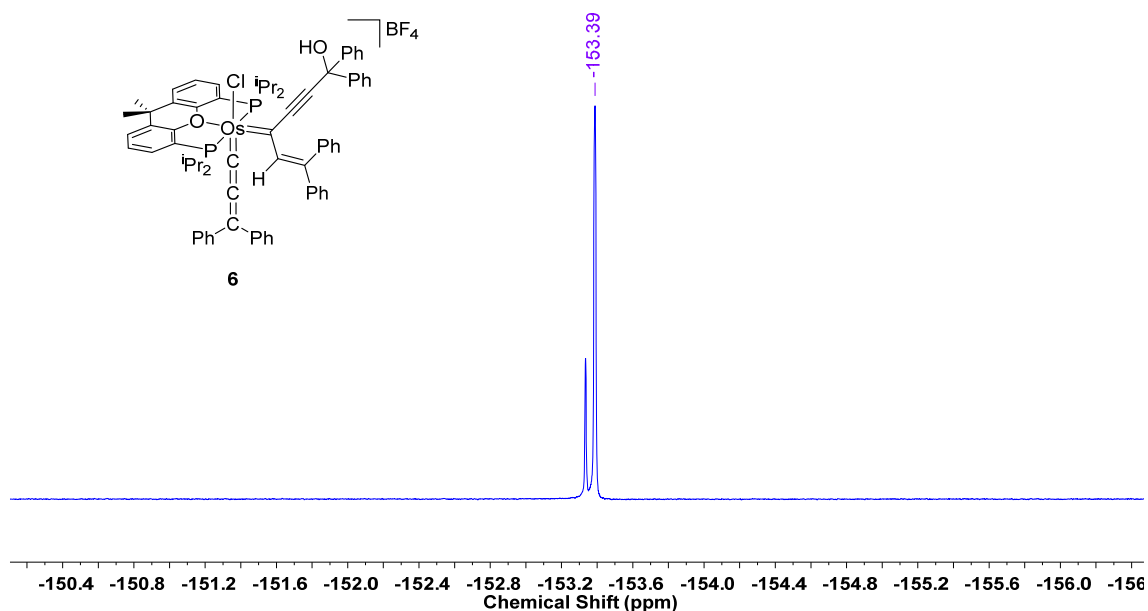


Figure S24. $^{19}\text{F}\{\text{H}\}$ NMR spectrum (282.38 MHz, CD_2Cl_2 , 298 K) of **6**.

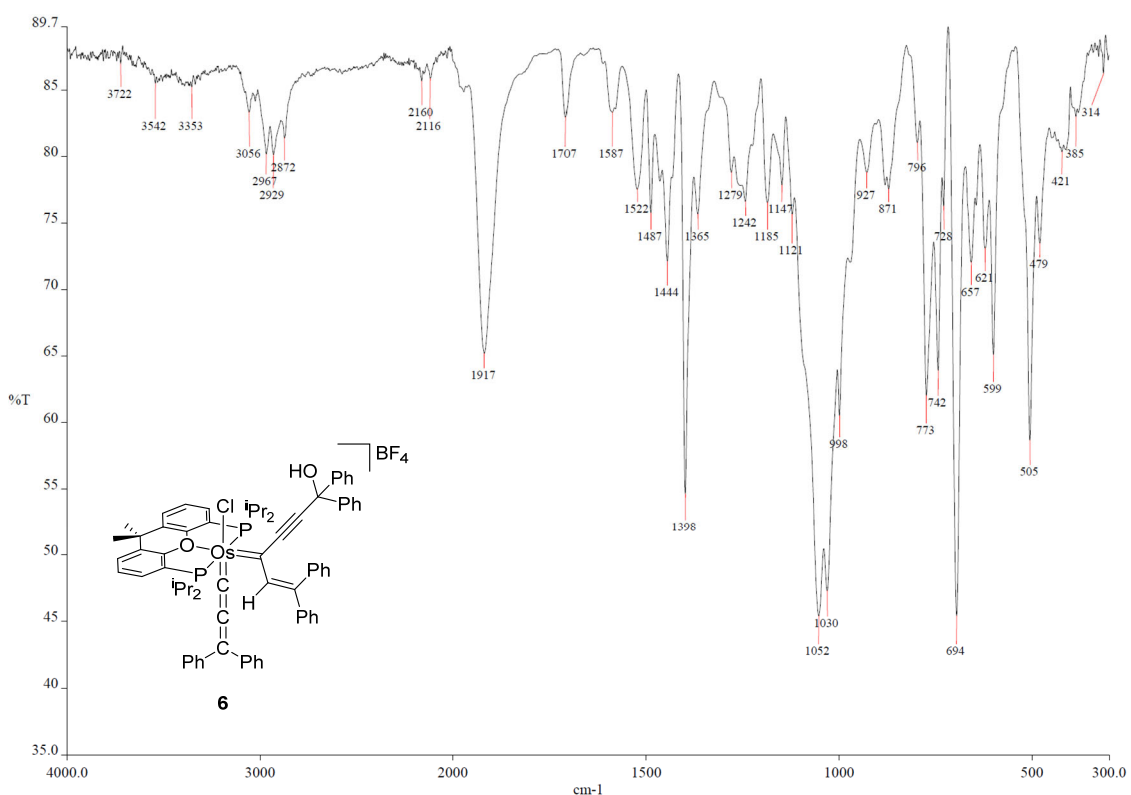


Figure S25. ATR-IR spectrum of **6**.

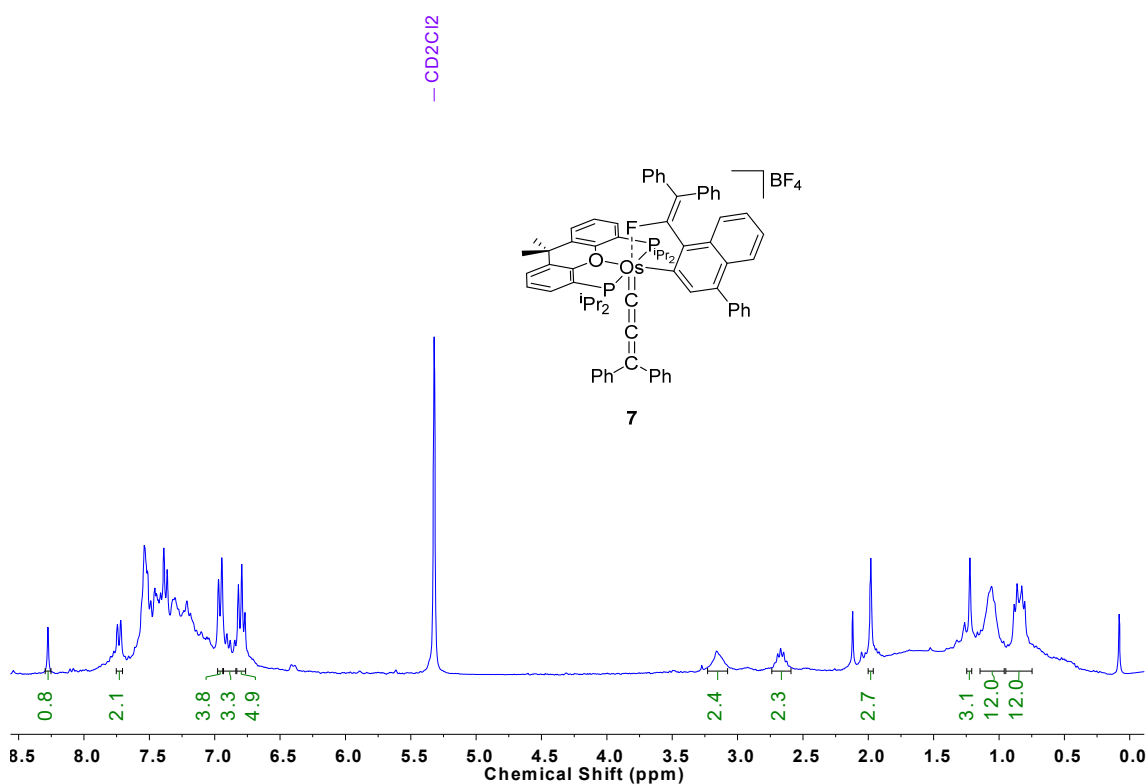


Figure S26. ¹H NMR spectrum (300.13 MHz, CD₂Cl₂, 298 K) of **7**.

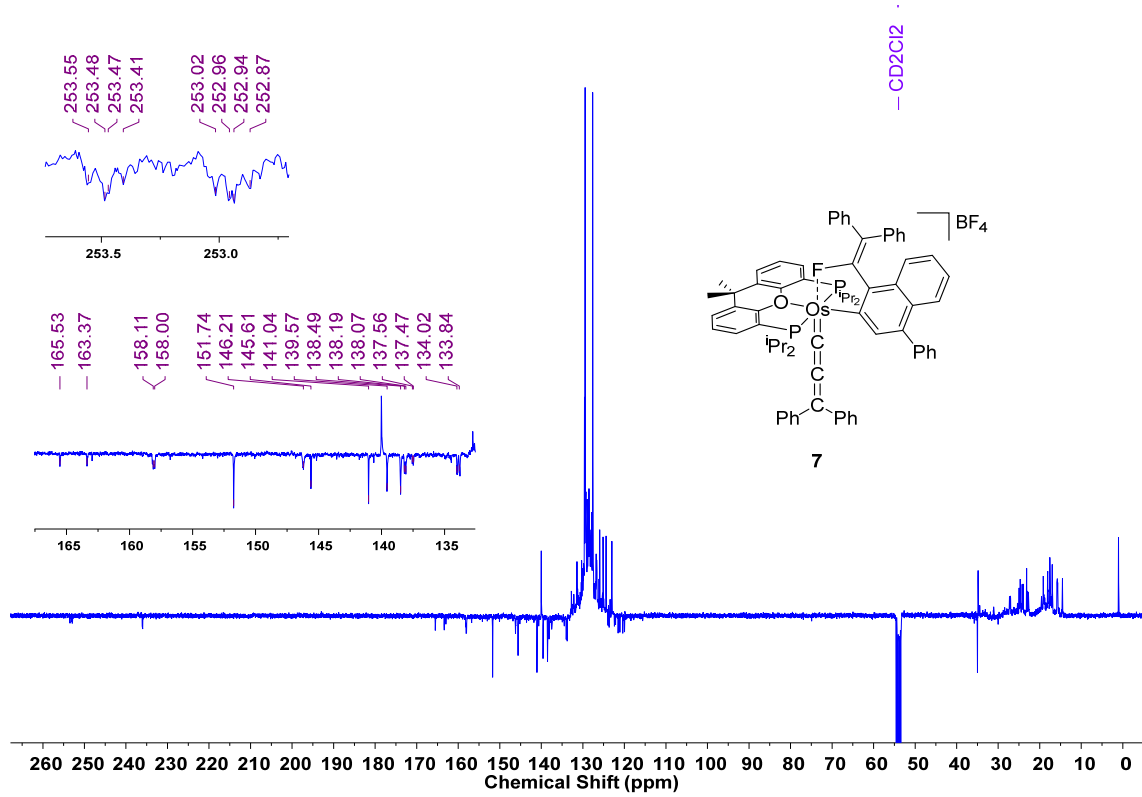


Figure S27. $^{13}\text{C}\{^1\text{H}\}$ -APT NMR spectrum (100.62 MHz, CD_2Cl_2 , 243 K) of **7**.

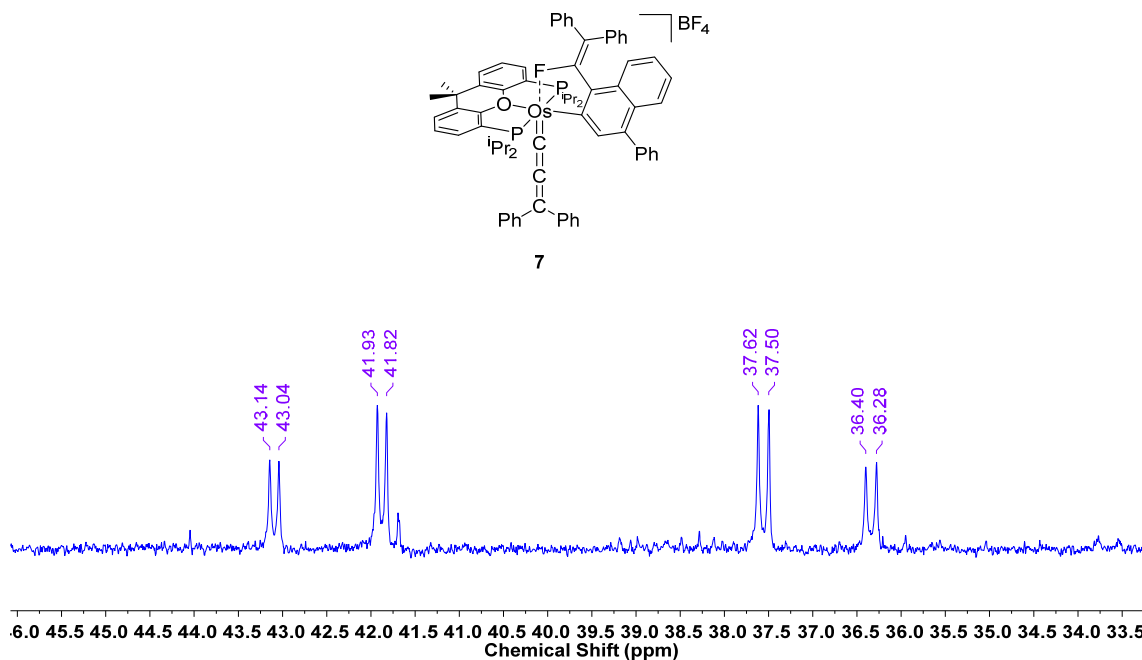


Figure S28. $^{31}\text{P}\{^1\text{H}\}$ NMR spectrum (161.98 MHz, CD_2Cl_2 , 243 K) of **7**.

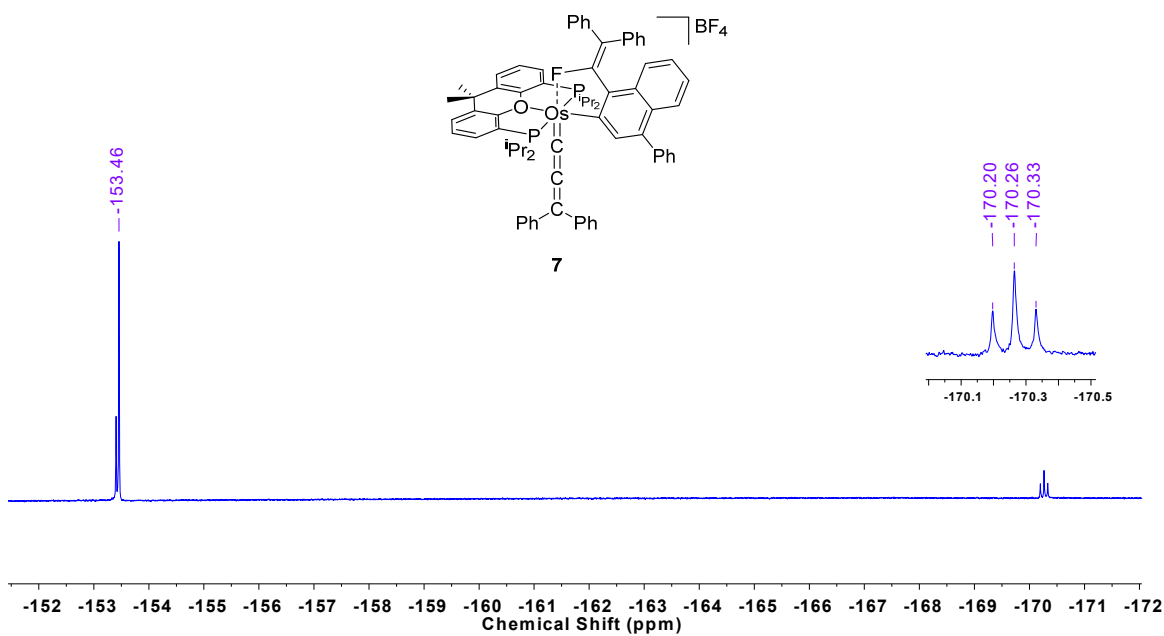


Figure S29. $^{19}\text{F}\{^1\text{H}\}$ NMR spectrum (282.38 MHz, CD_2Cl_2 , 298 K) of 7.

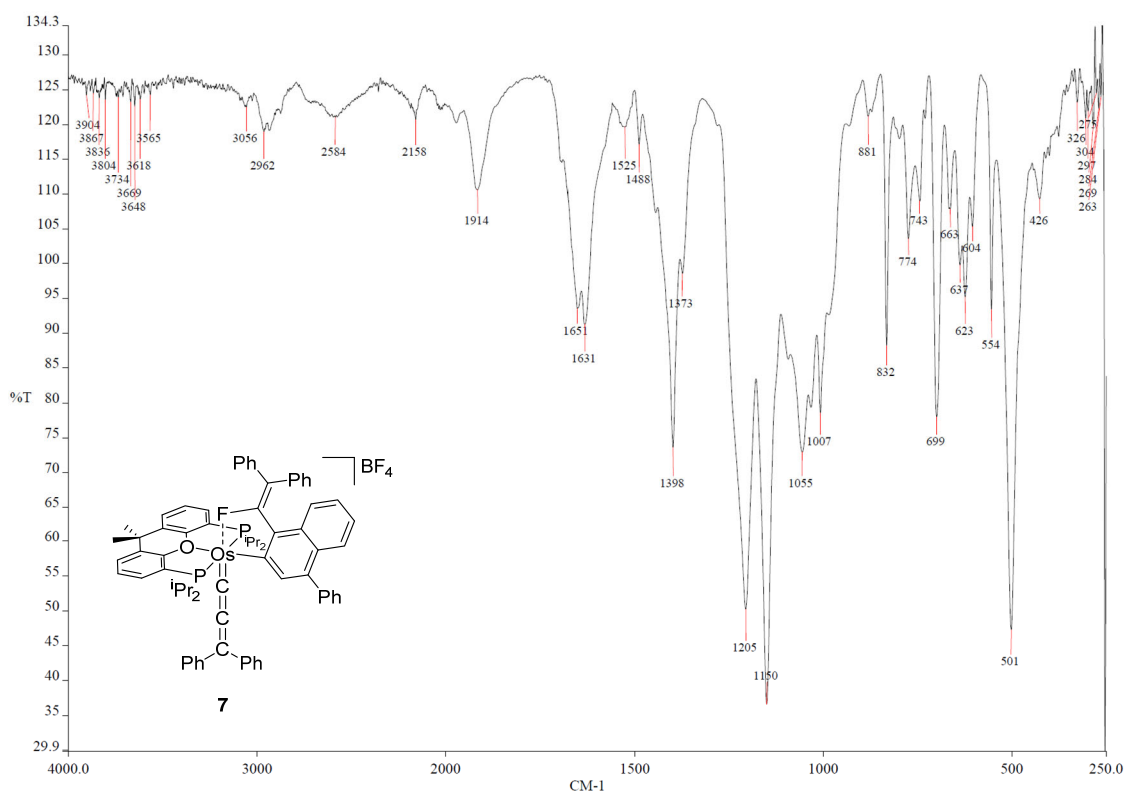


Figure S30. ATR-IR spectrum of 7.

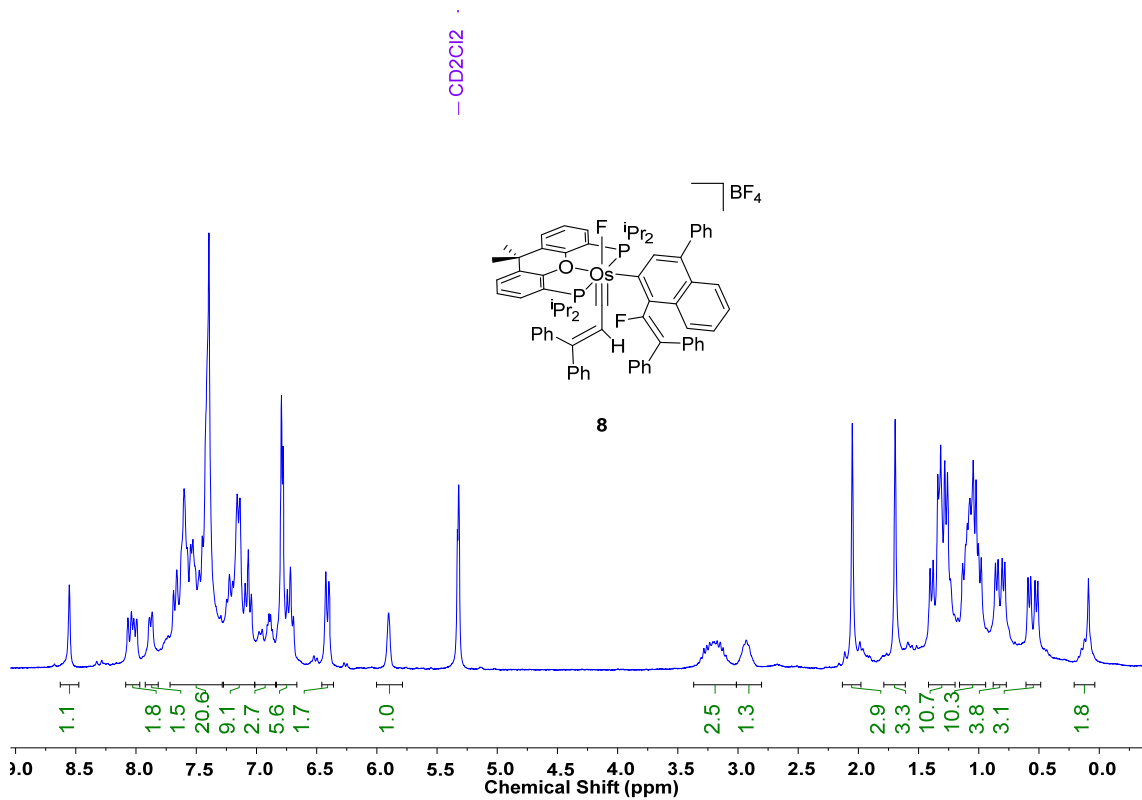


Figure S31. ^1H NMR spectrum (300.13 MHz, CD₂Cl₂, 298 K) of **8**.

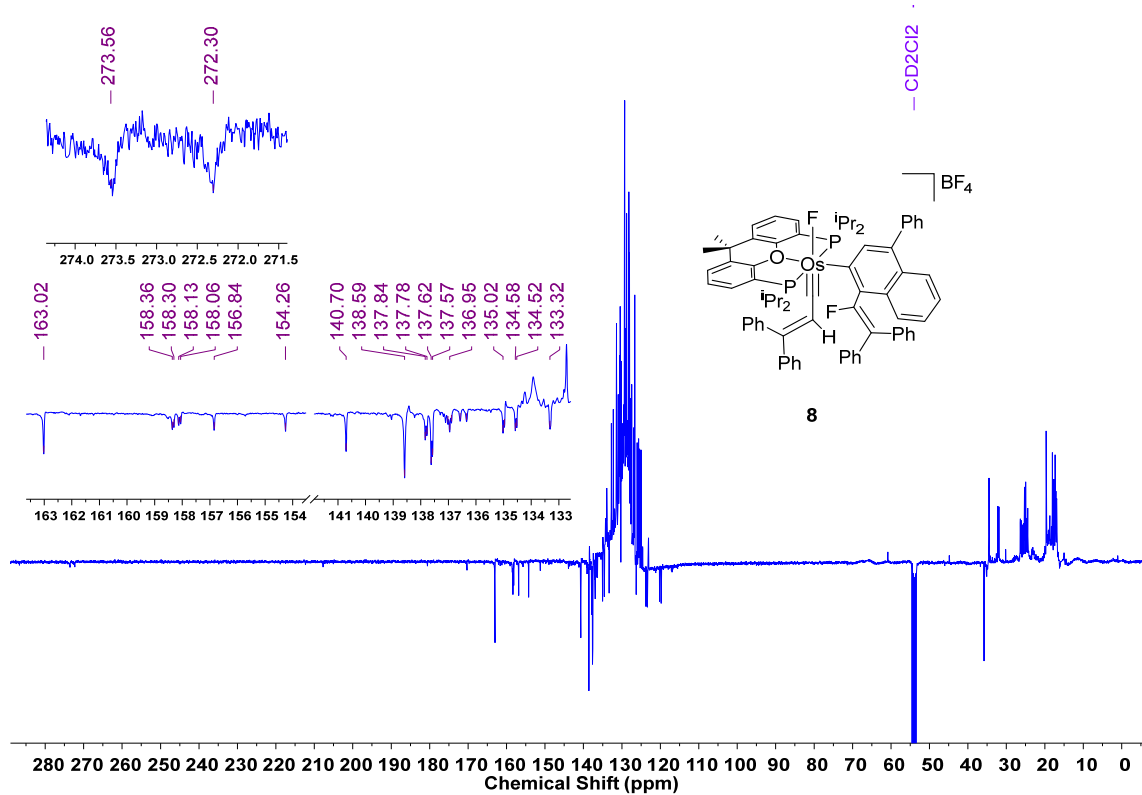


Figure S32. $^{13}\text{C}\{^1\text{H}\}$ -APT NMR spectrum (100.62 MHz, CD₂Cl₂, 253 K) of **8**.

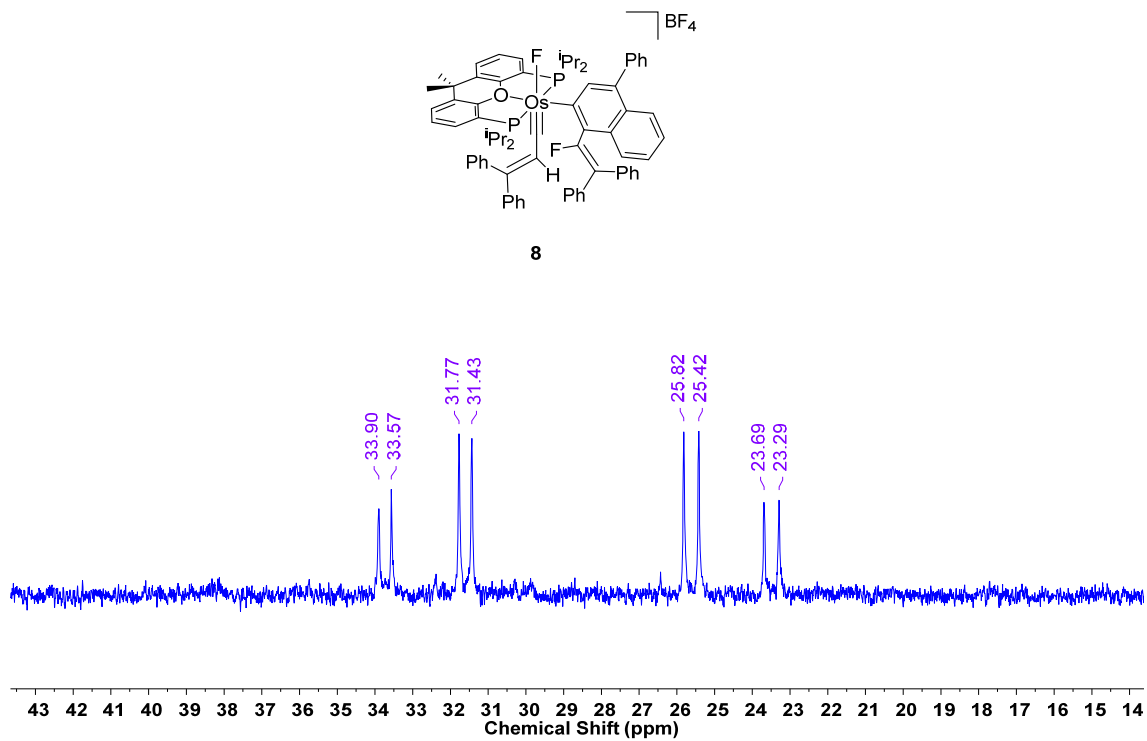


Figure S33. $^{31}\text{P}\{\text{H}\}$ NMR spectrum (121.49 MHz, CD_2Cl_2 , 298 K) of **8**.

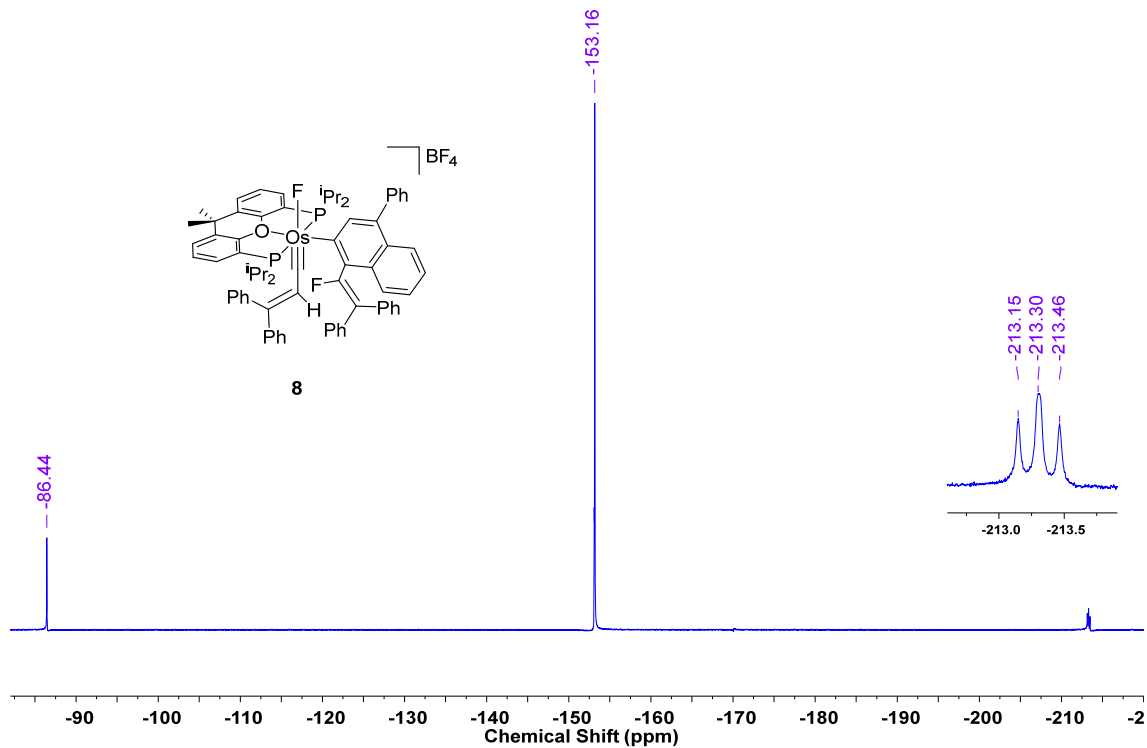


Figure S34. $^{19}\text{F}\{\text{H}\}$ NMR spectrum (282.38 MHz, CD_2Cl_2 , 298 K) of **8**.

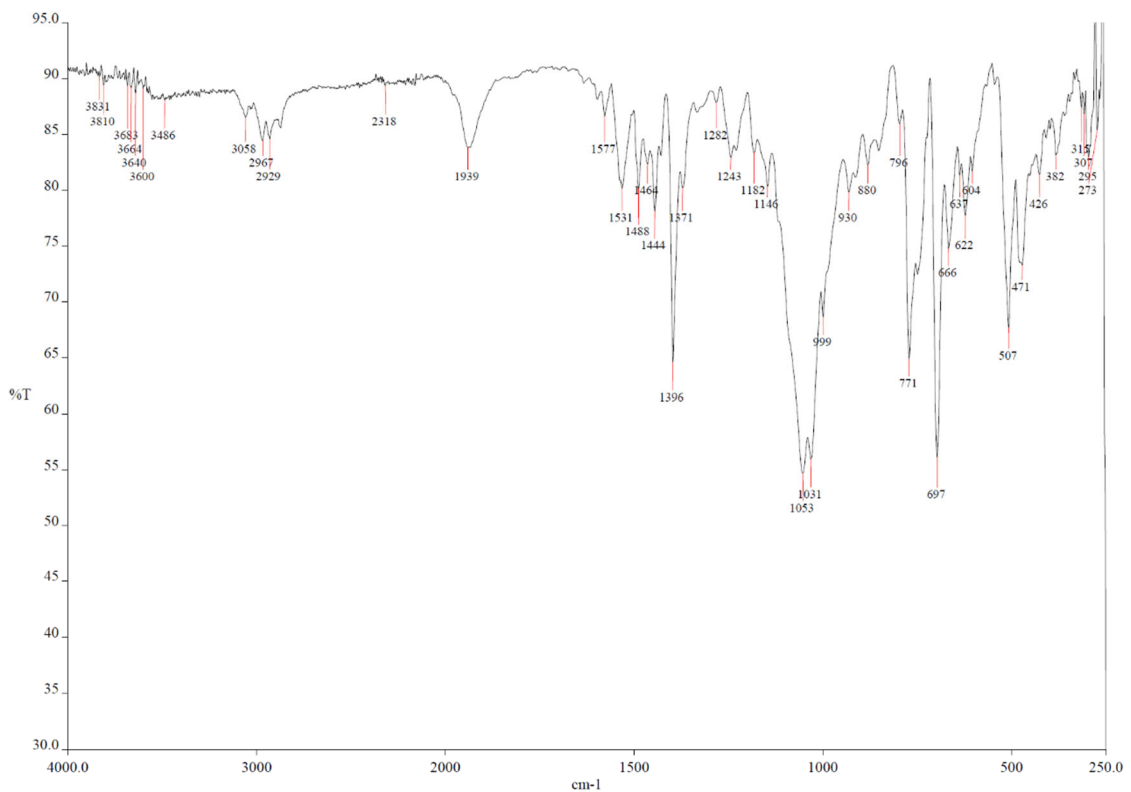


Figure S35. ATR-IR spectrum of **8**.

– References

- (1) Babón, J. C.; Esteruelas, M. A.; Oñate, E.; Paz, S.; Vélez, A. Silyl-Osmium(IV)-Trihydride Complexes Stabilized by a Pincer Ether-Diphosphine: Formation and Reactions with Alkynes. *Organometallics* **2022**, *41*, 2022–2034.
- (2) Blessing, R. H. *Acta Crystallogr.* **1995**, *A51*, 33. SADABS: Area-detector absorption correction; Bruker- AXS, Madison, WI, 1996.
- (3) SHELXL-2018/3 Sheldrick, G. M. *Acta Cryst.* **2008**, *A64*, 112–122.
- (4) (a) Lee, C.; Yang, W.; Parr, R. G. Development of the Colle-Salvetti correlationenergy formula into a functional of the electron density. *Phys. Rev. B* **1988**, *37*, 785–789. (b) Becke, A. D. Density-functional exchange-energy approximation with correct asymptotic behavior. *J. Chem. Phys.* **1993**, *98*, 5648–5652. (c) Stephens, P. J.; Devlin, F. J.; Chabalowski, C. F.; Frisch, M. J. Ab Initio Calculation of Vibrational Absorption and Circular Dichroism Spectra Using Density Functional Force Fields. *J. Phys. Chem.* **1994**, *98*, 11623–11627.
- (5) Grimme, S.; Antony, J.; Ehrlich, S.; Krieg, H. A consistent and accurate ab initio parametrization of density functional dispersion correction (DFT-D) for the 94 elements H-Pu. *J. Chem. Phys.* **2010**, *132*, 154104–154123.
- (6) Gaussian 09, Revision D.01, Frisch, M. J.; Trucks, G. W.; Schlegel H. B.; Scuseria, G. E.; Robb, M. A.; Cheeseman, J. R.; Scalmani, G.; Barone, V.; Mennucci, B.; Petersson, G. A.; Nakatsuji, H.; Caricato, M.; Li, X.; Hratchian, H. P.; Izmaylov, A. F.; Bloino, J.; Zheng, G.; Sonnenberg, J. L.; Hada, M.; Ehara, M.; Toyota, K.; Fukuda, R.; Hasegawa, J.; Ishida, M.; Nakajima, T.; Honda, Y.; Kitao, O.; Nakai, H.; Vreven, T.; Montgomery, J. A.; Peralta, Jr., J. E.; Ogliaro,

F.; Bearpark, M.; Heyd, J. J.; Brothers, E.; Kudin, K. N.; Staroverov, V. N.; Keith, T.; Kobayashi, R.; Normand, J.; Raghavachari, K.; Rendell, A.; Burant, J. C.; Iyengar, S. S.; Tomasi, J.; Cossi, M.; Rega, N.; S43 Millam, J. M.; Klene, M.; Knox, J. E.; Cross, J. B.; Bakken, V.; Adamo, C.; Jaramillo, J.; Gomperts, R.; Stratmann, R. E.; Yazyev, O.; Austin, A. J.; Cammi, R.; Pomelli, C.; Ochterski, J. W.; Martin, R. L.; Morokuma, K.; Zakrzewski, V. G.; Voth, G. A.; Salvador, P.; Dannenberg, J. J.; Dapprich, S.; Daniels, A. D.; Farkas, O.; Foresman, J. B.; Ortiz, J. V.; Cioslowski, J.; Fox, D. J. Gaussian, Inc., Wallingford CT, 2013.

- (7) Andrea, D.; Häußermann, U. M.; Dolg, M.; Stoll, H.; Preuss, H. Energyadjusted ab initio pseudopotentials for the second and third row transition elements. *Theor. Chim. Acta* **1990**, *77*, 123–141.
- (8) Ehlers, A. W.; Bohme, M.; Dapprich, S.; Gobbi, A.; Hollwarth, A.; Jonas, V.; Kohler, K. F.; Stegmann, R.; Veldkamp, A.; Frenking, G. A set of f-polarization functions for pseudo-potential basis sets of the transition metals SC-Cu, Y-Ag and La-Au. *Chem. Phys. Lett.* **1993**, *208*, 111–114.
- (9) (a) Hehre, W. J.; Ditchfield, R.; Pople, J. A. Self-Consistent Molecular Orbital Methods. XII. Further Extensions of Gaussian-Type Basis Sets for Use in Molecular Orbital Studies of Organic Molecules. *J. Chem. Phys.* **1972**, *56*, 2257–2261. (b) Franch, M. M.; Pietro, W. J.; Hehre, W. J.; Binkley, J. S.; Gordon, M. S.; DeFrees, D. J.; Pople, J. A. Self-consistent molecular orbital methods. XXIII. A polarization-type basis set for second-row elements. *J. Chem. Phys.* **1982**, *77*, 3654–3665.